

Discovery of a New Class of Natural Product-Inspired Quinazolinone Hybrid as Potent Antileishmanial agents

Moni Sharma,^{†,‡} Kuldeep Chauhan,[†] Rahul Shivahare,[§] Preeti Vishwakarma,[§] Manish K. Suthar,^{||} Abhishek Sharma,[⊥] Suman Gupta,[§] Jitendra K. Saxena,^{||} Jawahar Lal,[⊥] Preeti Chandra,[#] Brijesh Kumar,[#] and Prem M. S. Chauhan^{*,†}

[†]Medicinal and Process Chemistry Division, CSIR—Central Drug Research Institute, Lucknow-226 001, U.P., India

[‡]Department of Chemistry, Bhagwant University, Ajmer, India

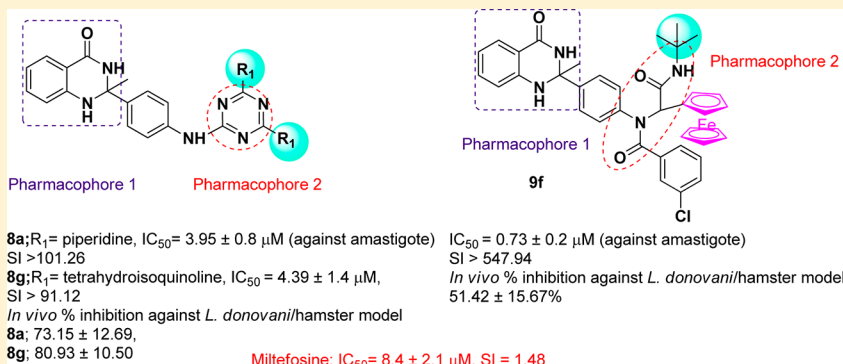
[§]Division of Parasitology, CSIR—Central Drug Research Institute, Lucknow-226 001, U.P., India

^{||}Division of Biochemistry, CSIR—Central Drug Research Institute, Lucknow-226 001, U.P., India

[⊥]Pharmacokinetics & Metabolism Division, CSIR—Central Drug Research Institute, Lucknow-226 001, U.P., India

[#]Sophisticated Analytical Instrumentation Facility, CSIR—Central Drug Research Institute, Lucknow 226001, India

Supporting Information



ABSTRACT: The high potential of quinazolinone containing natural products and their derivatives in medicinal chemistry led us to discover four novel series of 53 compounds of quinazolinone based on the concept of molecular hybridization. Most of the synthesized analogues exhibited potent leishmanicidal activity against intracellular amastigotes (IC₅₀ from 0.65 ± 0.2 to 7.76 ± 2.1 μM) as compared to miltefosine (IC₅₀ = 8.4 ± 2.1 μM) and nontoxic toward the J-774A.1 cell line and Vero cells. Moreover, activation of Th1 type and suppression of Th2 type immune responses and induction in nitric oxide generation proved that **8a** and **8g** induce murine macrophages to prevent survival of parasites. Compounds **8a** and **8g** exhibited significant *in vivo* inhibition of parasite 73.15 ± 12.69% and 80.93 ± 10.50% against *Leishmania donovani*/hamster model. Our results indicate that compounds **8a**, **8g**, and **9f** represent a new structural lead for this serious and neglected disease.

INTRODUCTION

Leishmaniasis is a debilitating disease caused by the protozoan parasites of the genus *Leishmania* that pose serious public health challenges for prevention, diagnosis, and treatment.¹ *Leishmania donovani*, the etiologic agent of visceral leishmaniasis (VL), affects about 12 million people in nearly 90 countries and an estimated 51000 annual deaths for leishmaniasis, representing a significant health problem in tropical and subtropical regions of the world.² *Leishmania* parasites are transmitted to humans almost exclusively by biting of infected phlebotomine sand flies as proliferative promastigotes. Inside the mammalian body, the parasite multiplies within phagolysosomes of macrophages as intracellular amastigotes.³ Active VL is almost fatal if not treated after the onset of clinicopathological abnormalities.⁴ To survive within macrophages, *Leishmania* has developed several mecha-

nisms to cause dysfunction in their host macrophages and the outcome of infection depends on the production and/or secretion of immunosuppressive molecules that includes transforming growth factor (TGF)-β, interleukin (IL)-10, and prostaglandin E2 (PGE2).^{5a} These molecules distort the normal immune response by suppression of host-protective microbicidal molecules, nitric oxide (NO), and reactive oxygen species (ROS) and cytokines interferon (IFN)-γ, IL-1, IL-12, and tumor necrosis factor-α (TNF-α).^{5b} Antileishmanial therapy relies on handful number of drugs such as antimony-based drugs: meglumine antimoniate (Glucantime), sodium stibogluconate (Pentostam), pentamidine, amphotericin B, and miltefosine.⁶

Received: January 11, 2013

Published: April 23, 2013

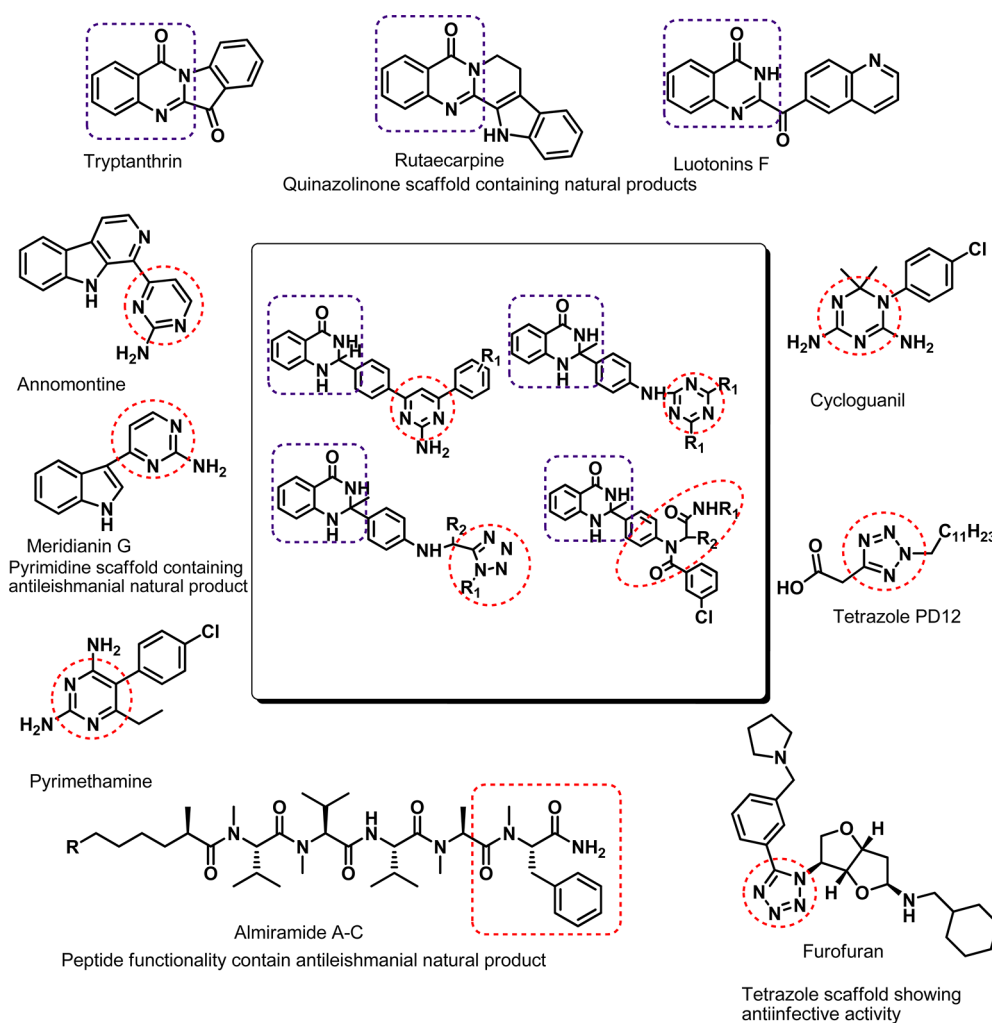


Figure 1. Designing of quinazolinone-based hybrids showing antileishmanial activity.

Pentavalent antimony, a prodrug which was developed before 1959, is characterized by high toxicity and limited efficacy. Conventional amphotericin B as the first-line treatment for VL has replaced antimonials in some areas of the Bihar State of India where more than 60% of newly diagnosed VL cases in this area do not respond to antimonials.⁷ Pentamidine (an aromatic diamidine), the second line treatment options for VL, is also far from satisfactory due to several side effects and not active orally. WHO/TDR is currently developing a research program with miltefosine (a teratogenic drug), represents a fundamental advance in antileishmanial chemotherapy because it is the first oral agent. Despite its great efficacy, this drug has a long half-life (more than 150 h) and parasite resistance is easily induced in vitro, therefore its use is strictly outlawed in pregnant women.⁸ Because most of the drugs used in treatment have a list of problems like unaffordable cost, difficulty in administration, high toxicity, and more importantly the resistance problem.⁹ In view of the foregoing facts, the search for innovative drugs based on new molecular scaffolds that target the specific metabolic pathway of the parasite should be highly prioritized, which in turn requires new medicinal chemistry approaches to discover novel lead compounds that might populate a pipeline of new therapeutics. Unfortunately, our limited discerning of leishmania biology makes difficult the rational designing of antileishmanial agents.

An attractive concept of hybridization for neglected tropical disease is becoming popular as an emerging structural modification tool to design new molecules with improved bioactivity when compared to the parent compounds.^{10–12} In this context, biology oriented synthesis (BIOS) of natural product-inspired scaffolds and their hybrids may show promising results in finding new lead structures for chemical biology and medicinal chemistry research.^{13–15} Furthermore, bioactive small molecule natural products possess all of the potency, selectivity, and pharmacokinetic persona, an important paradigm for drug-like molecules.¹⁶ However, the number of natural products are limited, hence incorporating either different natural products or drug fragments may provide millions of combinations which will be enriched in biological activity and less toxicity.

Quinazolinone is a building block of naturally occurring alkaloids and is utilized as a druglike scaffold in several natural products^{17–21} (trypanthrin, rutaecarpine, and luotonin A, Figure 1), as these possess a wide range of biological activities including antitumor,²² anticonvulsant,²² antiviral,²³ anti-inflammatory, analgesic,²⁴ antimicrobial,²⁵ antifungal,²⁶ antimalarial,²⁷ antidiabetic,²⁸ cytotoxicity,²⁹ and angiotensin II AT1 receptor antagonists.³⁰ Recently, we have developed an efficient and facile methodology for the preparation of this privileged scaffold.³¹

On the other hand, among the different heterocyclic structures that have been disclosed, the nitrogen containing class of

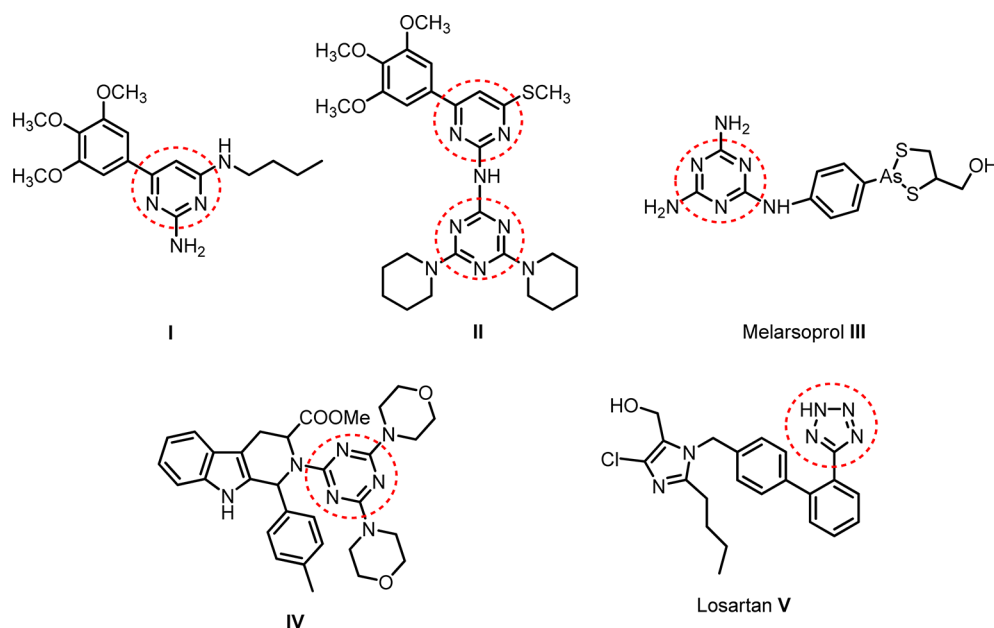


Figure 2. Examples of some pyrimidine-, triazine-, and tetrazole-based bioactive agents.

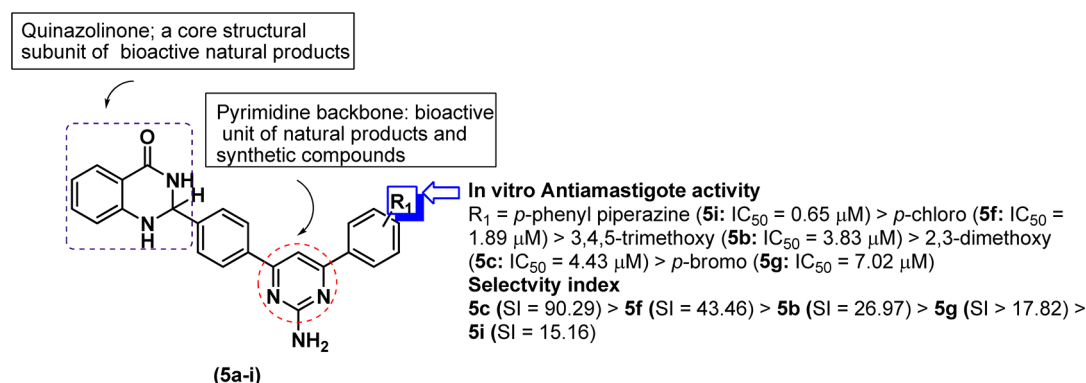


Figure 3. SAR of the synthesized quinazolinone-pyrimidine hybrids.

compounds such as pyrimidine, triazine, peptide, and tetrazole that are found in many natural products (annonentine, meridianin G, and almiramide A–C)^{32–34} are the important constituents of number of modern drugs^{35–37} (Figures 1 and 2). Interestingly, some of these from natural sources have been screened as potent antileishmanial agents and a number of them exhibited multifarious pharmacological profiles (Figure 1).^{38–40} Moreover, previously we have reported the pyrimidine and triazine class of analogues as good antileishmanial agents (Figure 2).⁴¹

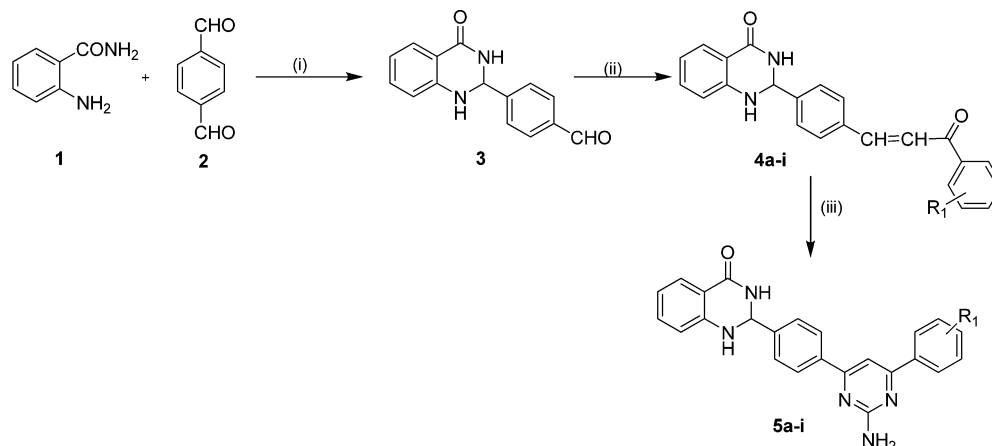
On the basis of this reasoning and as a part of our ongoing interest toward the design and synthesis of novel heterocycles as anti-infective agents,⁴² we have synthesized the quinazolinone hybrids via introducing heterocyclic systems as discussed above with different possible functionalities. To the best of our knowledge, the hybridization of these bioactive pharmacophores and their antileishmanial activity has never been reported to date. Through these processes, we have discovered novel scaffolds with potent antileishmanial activity with a high selective index which was comparable or superior to other current antileishmanials, miltefosine and SSG (sodium stibogluconate). The compounds which have a combination of high efficacy and no cytotoxicity with the high value of selective index were tested for in vivo study in a chronic hamster model. We also investigated

the interaction of the most potent compounds with bovine serum albumin (BSA). Serum albumin, major soluble blood protein, has many physiological functions such as maintenance of colloidal osmotic pressure and blood pH. Another characteristic property of albumins is their reversible interactions with various endogenous and exogenous compounds which facilitate the transportation and disposition of several compounds including drugs, proteins, and fatty acids to specific targets.^{43–45} BSA a 66 kDa monomer having domains and subdomains stabilized by 17 pairs of disulfide bridges shows 80% structural homology with human serum albumin.^{46–48}

RESULTS AND DISCUSSION

Chemistry. To realize a facile access toward quinazolinone hybrids with various bioactive heterocycles from readily available substrates, a set of compounds were synthesized for the structure–activity relationship (SAR).

Synthesis of Quinazolinone–Pyrimidines (5a–i, Figure 3). 4-(4-Oxo-1,2,3,4-tetrahydroquinazolin-2-yl)benzaldehyde (3)³¹ and various substituted acetophenones were subjected to Claisen–Schmidt condensation⁴⁹ using KOH in ethanol to afford the corresponding quinazolinone–chalcones (4a–i). Intermediate (4a–i) were reacted with the guanidine hydro-

Scheme 1. Synthesis of Quinazolinone–Pyrimidine Derivatives (5a–i)^a

^aReagents and conditions: (i) cyanuric chloride, CH₃CN, 15 min; (ii) substituted acetophenone, KOH, EtOH, 5h rt; (iii) guanidine hydrochloride, NaH, DMF, 70 °C, 5 h.

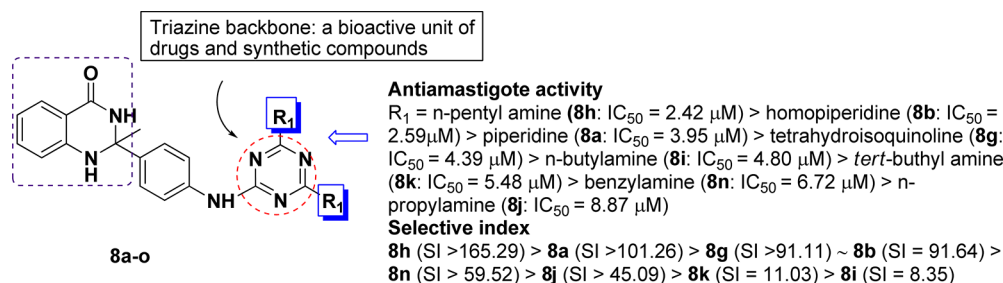
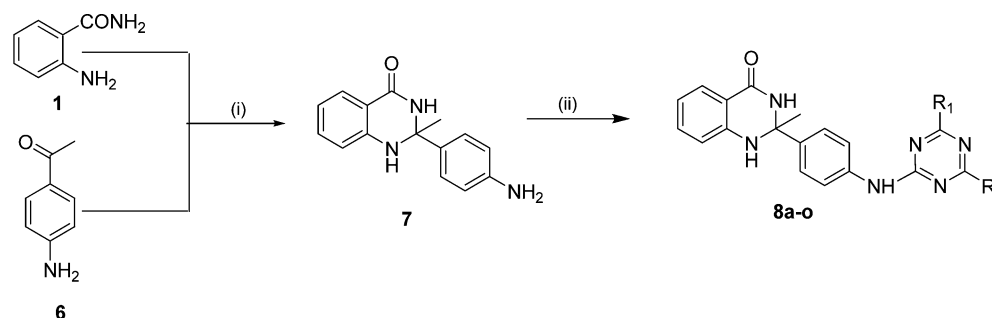


Figure 4. SAR of the synthesized quinazolinone–triazine hybrids.

Scheme 2. Synthesis of Quinazolinone–Triazine Derivatives (8a–o)^a

^aReagents and conditions: (i) acidic SiO₂, dry MeOH, 3 h, 60 °C; (ii) (a) cyanuric chloride, THF, 1 h rt; (b) various amines, K₂CO₃, DMF, reflux, 4 h.

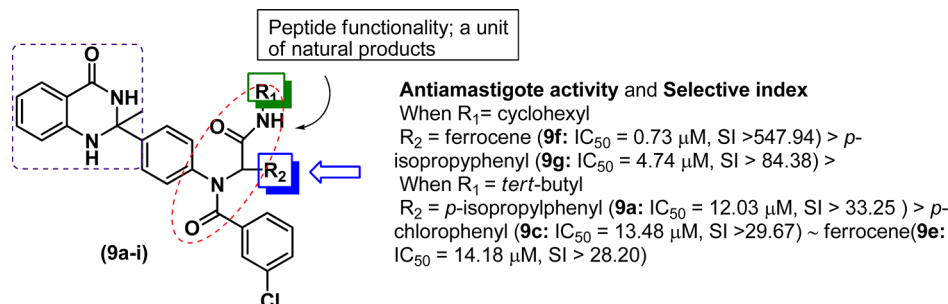


Figure 5. SAR of the synthesized quinazolinone–peptide hybrids.

chloride in the presence of NaH in DMF to afford the target quinazolinone–pyrimidines (5a–i, Scheme 1).

Synthesis of Quinazolinone–Triazine (8a–r, Figure 4). For the scope of the quinazolinone hybrid, introduction of 1,3,5-

Scheme 3. Synthesis of Quinazolinone–Peptide Derivatives (9a–i)

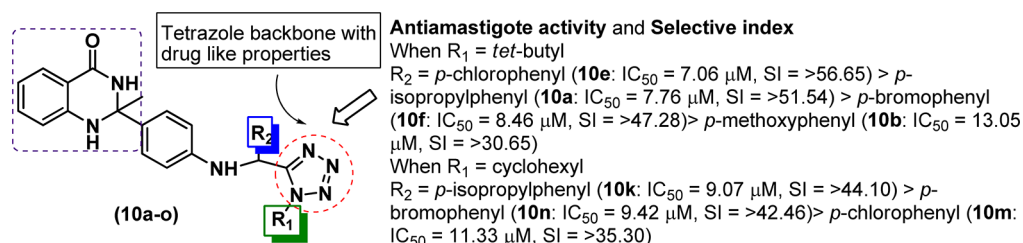
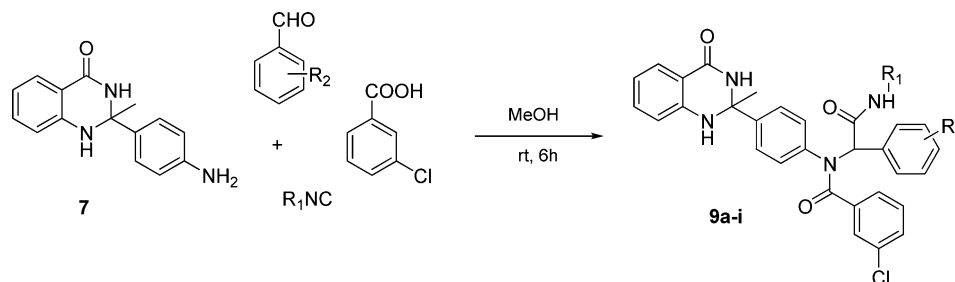
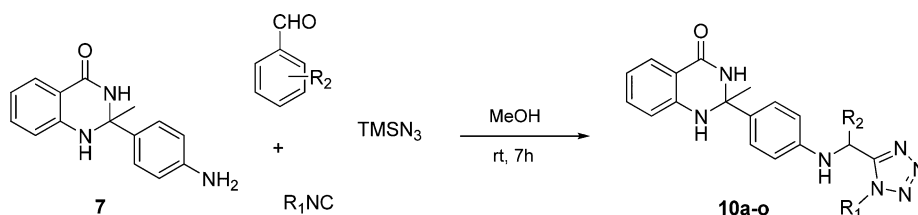
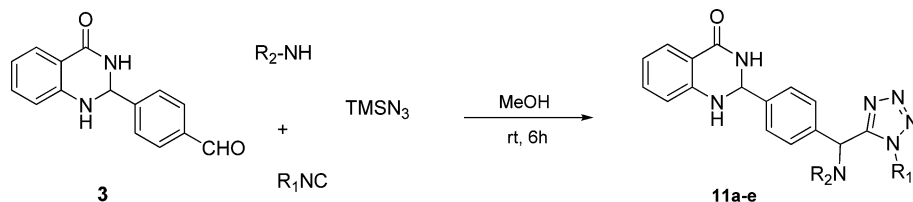


Figure 6. SAR of the synthesized quinazolinone–tetrazole hybrids.

Scheme 4. Synthesis of Quinazolinone–Tetrazole Derivatives (10a–o)



Scheme 5. Synthesis of Quinazolinone–Tetrazole Derivatives (11a–e)



triazine at the quinazolinone ring was envisaged. In this respect, a straightforward synthetic approach was followed for the synthesis of compounds (**8a–r**, Scheme 2). The synthesis of 2,4,6-trisubstituted-[1,3,5]triazines were achieved by consecutive nucleophilic substitution of cyanuric chloride. The whole sequence is performed in the same pot with the change of solvent. Quinazolinone–triazine analogues (**8a–r**) were formed by nucleophilic substitution of cyanuric chloride and 2-(4-aminophenyl)-2-methyl-2,3-dihydroquinazolin-4(1H)-one (**7**) in THF at room temperature followed by treatment with various amines using K_2CO_3 in dry DMF at 70 °C. Compound **7** was prepared by the acidic silica-catalyzed condensation of commercially available anthralinamide (**1**) and *p*-aminoacetophenone (**6**) in MeOH at 60 °C.

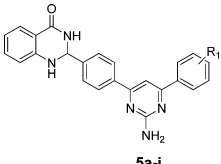
Synthesis of Quinazolinone–Peptide (9a–i, Figure 5). Because the isocyanide-based multicomponent reactions (IMCRs) are considered as powerful tools in modern organic synthesis and drug discovery,⁵⁰ therefore, to further optimize the SAR, the preparation of new chemical entities (NCEs), based on multicomponent Ugi reaction, was designed for the creation of quinazolinone–peptides. The 2-(4-aminophenyl)-2-methyl-2,3-

dihydroquinazolin-4(1H)-one (**7**), *m*-chlorobenzoic acid, various commercially available aldehydes, and different isocyanides were subjected to IMCRs in methanol to afford the corresponding quinazolinone–peptides (**9a–i**, Scheme 3) with good to excellent yield at room temperature.

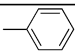
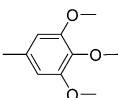
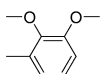
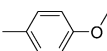
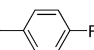
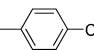
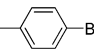
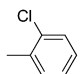
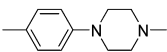
Synthesis of Quinazolinone–Tetrazole (10a–o, 11a–e). To further optimize the quinazolinone analogues, we have synthesized a series of quinazolinone–tetrazoles (**10a–o**) for generating the collections of molecules with high molecular diversity via modified $TMSN_3$ –Ugi MCR (Figure 6).^{50b} In this context, compound **7** was allowed to react at room temperature with different commercially available aldehydes, isocyanides, and azidotrimethylsilane ($TMSN_3$) in anhydrous methanol to form the desired quinazolinone–tetrazoles (**10a–o**, Scheme 4) in good to excellent yield at room temperature. To introduce further diversity in the quinazolinone–tetrazole hybrids for the SAR, we have designed and synthesized another series of quinazolinone–tetrazole analogue (**11a–e**) as shown in Scheme 5.

The structures of the compounds were substantiated by 1H NMR, ^{13}C NMR, mass spectrometry and IR spectroscopy.

Table 1. In Vitro Antileishmanial Activity of Quinazolinone–Pyrimidine (5a–i)



5a-i

Entry	R1	Anti-promastigote activity IC ₅₀ (μM)	Anti-amastigote activity IC ₅₀ ^a (μM)	Cytotoxicity ^b CC ₅₀ (μM) on J-774A.1 cell line	Cytotoxicity CC ₅₀ (μM) on vero cell line	Selectivity Index ^c (SI)
5a		4.04 ± 1.2	17.00 ± 2.1	ND ^d	ND	NA ^e
5b		3.44 ± 0.9	3.83 ± 1.1	103.32 ± 8.5	85.86 ± 8.8	26.97
5c		4.23 ± 1.2	4.43 ± 1.5	>400	>400	90.29
5d		5.79 ± 1.3	10.08 ± 1.4	177.86 ± 9.8	124.33 ± 14.6	17.64
5e		9.83 ± 1.2	24.68 ± 2.3	ND	ND	NA
5f		3.07 ± 1.3	1.89 ± 0.9	82.15 ± 5.5	322.72 ± 15.6	43.46
5g		2.82 ± 1.2	7.02 ± 1.5	125.12 ± 6.8	>400	17.82
5h		9.00 ± 2.5	15.31 ± 2.3	ND	ND	NA
5i		1.75 ± 0.9	0.65 ± 0.2	10.15 ± 2.5	8.32 ± 2.2	15.16

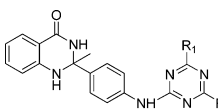
^aIC₅₀ values are the average of two independent assays expressed as average ± standard error. ^bCC₅₀ on J-774A.1 cells. ^cThe selectivity index (SI) is defined as the ratio of CC₅₀ on J-774A.1 cells from (^b) to IC₅₀ on *L. donovani* intracellular amastigotes (^a). ^dND: not determined. ^eNA: not available.

Biological Activity. In an attempt to identify novel quinazolinone hybrids, a novel series of 53 compounds was subjected to the screening test against *L. donovani*. Each candidate was evaluated for its in vitro activity against WHO reference strain (MHOM/IN/80/Dd8) of extracellular promastigotes⁴ and intramacrophagic amastigotes (expressing luciferase firefly reporter gene) of *L. donovani*.⁵¹ The in vitro cytotoxicity assay was performed using murine macrophage cells (J-774A.1 cell line) and mammalian kidney fibroblast cells (Vero cell line).⁵² The selectivity of a compound was defined as the ratio of the cytotoxicity in macrophage cells and the inhibitory activity in intracellular amastigotes. Compounds which showed in vitro potency with high selectivity were further tested for their in vivo efficacy in golden hamsters at a dosage of 50 mg/kg for five days through the intraperitoneal (IP) route.⁵³ Standard antileishmanials, miltefosine and SSG, were included in the study as control drugs. SARs of the quinazolinone hybrids have been extensively studied with the different counterparts and wide variation of substituents around it to optimize potency/selectivity. The intracellular amastigote form is the clinically relevant parasitic stage for biological evaluation and interestingly, we were very pleased to find that among the synthesized analogues most of the

analogues were more potent against intracellular amastigote form than promastigotes (Tables 1–4).

In Vitro Antileishmanial Activity of Quinazolinone–Pyrimidine. Initially, a series of quinazolinone–pyrimidines (5a–i) was synthesized (Scheme 1) and evaluated for their in vitro antileishmanial activity, and the results are shown in Table 1. All the synthesized hybrids in this series showed significant to moderate activity against promastigote with IC₅₀ ranging from 1.75 ± 0.9 to 4.23 ± 1.2 μM. Compounds **5b–e**, **5g**, and **5i** displayed the significant antiamastigote activity in the micromolar range better than that of miltefosine. Miltefosine and SSG have been evaluated under the same conditions, miltefosine displayed significant antipromastigote (IC₅₀ = 1.05 ± 0.2 μM), moderate antiamastigote activity (IC₅₀ = 8.4 ± 2.1 μM), and toxic to the J-774A.1 cell line (CC₅₀ values of 12.42 ± 3.2 μM) and less cytotoxicity toward Vero cells (CC₅₀ values of 52.47 ± 2.4 μM). SSG displayed a poor antiamastigote activity (IC₅₀ = 46.70 ± 2.8 μM) although it is nontoxic to J-774A.1 (CC₅₀ 297.38 ± 10.2 μM) and Vero cells (CC₅₀ > 400 μM). Compound **5a**, which contained unsubstituted phenyl ring, was inactive against amastigotes. A progressive enhancement in antiamastigote potency was observed in the case of electron releasing substituents such as; 3,4,5-trimethoxy substituted hybrid (**5b**),

Table 2. In Vitro Antileishmanial Activity of Quinazolinone–Triazine (8a–o)



Entry	R ₁	Anti-promastigote activity IC ₅₀ (μM)	Anti-amastigote activity IC ₅₀ ^a (μM)	Cytotoxicity ^b CC ₅₀ (μM) on J-774A.1 cell line	Cytotoxicity CC ₅₀ (μM) on vero cell line	Selectivity Index ^c (SI)
8a		7.05 ± 2.3	3.95 ± 0.8	>400	>400	>101.26
8b		6.02 ± 2.4	2.59 ± 1.2	237.34 ± 11.5	>400	91.64
8c		>40	>40	ND	ND ^d	NA ^e
8d		>40	>40	ND	ND	NA
8e		>40	>40	ND	ND	NA
8f		33.17 ± 4.8	>40	ND	ND	NA
8g		>40	4.39 ± 1.4	>400	>400	>91.11
8h		7.46 ± 1.2	2.42 ± 0.9	>400	>400	>165.29
8i		7.69 ± 1.6	4.80 ± 1.1	40.09 ± 3.9	141.59 ± 7.4	8.35
8j		8.86 ± 2.1	8.87 ± 2.1	>400	>400	>45.09
8k		1.02 ± 0.4	5.48 ± 1.7	60.67 ± 5.1	159.16 ± 6.8	11.07
8l		13.20 ± 1.5	>20	ND	ND	NA
8m		3.02 ± 0.8	Toxic	ND	ND	NA
8n		6.38 ± 1.5	6.72 ± 1.1	>400	359.25 ± 12.5	>59.52
8o		>40	>40	ND	ND	NA

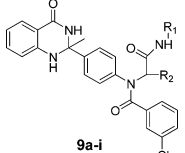
^aIC₅₀ values are the average of two independent assays expressed as average ± standard error. ^bCC₅₀ on J-774A.1 cells. ^cThe selectivity index (SI) is defined as the ratio of CC₅₀ on J-774A.1 cells (^b) to IC₅₀ on *L. donovani* intracellular amastigotes (^a). ^dND: not determined. ^eNA: not available.

displaying the promising activity (IC₅₀ = 3.83 ± 1.1 μM), followed by dimethoxy (5c, IC₅₀ = 4.43 ± 1.5 μM), and monomethoxy (5d, IC₅₀ = 10.08 ± 1.4 μM). Moreover, compounds 5b–d was nontoxic to the J-774A.1 cell line (CC₅₀ from 103.32 ± 8.5 to >400 μM) and Vero cells (85.86 ± 8.8 - >400 μM). Whereas compound 5c exhibited highest selectivity (SI = 90.29). The presence of the *p*-chloro substituent enhanced the antiamastigote activity of compound 5f (IC₅₀ = 1.89 ± 0.9 μM). Importantly, compound 5f was nontoxic to J-774A.1 and Vero cells (CC₅₀ = 82.15 ± 5.5 and 322.72 ± 15.6 μM, respectively). Having realized the importance of electron withdrawing groups on an aryl ring, we synthesized *o*-chloro substituted analogue 5h; unfortunately, antiamastigote activity was lost in 5h. With replacement of *p*-Cl with *p*-Br on the aryl ring (compound 5g), significant reduction in the antileishmanial activity was observed (IC₅₀ = 7.02 ± 1.5 μM), although it was nontoxic to J-774A.1 and Vero cells (CC₅₀ 125.12 ± 6.8 and >400 μM, respectively). However, in the *p*-fluoro substituted compound (5e), the antiamastigote activity was completely lost. Compound 5i, having *p*-phenylpiperazine substituent on the aryl ring of the R₁ group, was found to be the most active candidate with an IC₅₀ value of 0.65 ± 0.2 μM, 13-fold more potent than miltefosine (IC₅₀ = 8.4 ± 2.1 μM), however, its cytotoxicity was

high to both J-774A.1 and Vero cells (CC₅₀ value of 10.15 ± 2.5 and 8.32 ± 2.2 μM, respectively). Interestingly, most of the synthesized analogues exhibited better potency than the natural product (annomontine).

In Vitro Antileishmanial Activity of Quinazolinone–Triazine. To find out the role of the effect of triazine counterpart at the quinazolinone skeleton for SAR, quinazolinone–triazine hybrids (8a–o, Scheme 2) were prepared by varying the substituents around the triazine and screened for their in vitro antileishmanial activity (Table 2). Analogues 8b, 8k, 8m, and 8n displayed promising antipromastigote activity having IC₅₀ values in the range of 1.02 ± 0.4 to 6.38 ± 1.5 μM. Compounds 8a, 8b, 8g–i, 8k, and 8n exhibited more potent antiamastigote activity, having IC₅₀ values in the range of 2.42 ± 0.9 to 6.72 ± 1.1 μM than miltefosine. Compounds 8a–e, which have *p*-hydroxy piperidine, morpholine and aminopropyl morpholine were appeared to be inactive (IC₅₀ > 40 μM). Compound 8a, having piperidine substituents, exhibited significant activity (IC₅₀ = 3.95 ± 0.8 μM). Homopiperidine containing analogue 8b exhibited better activity (IC₅₀ = 2.59 ± 1.2 μM) than 8a. Both the analogues were nontoxic although 8a showed higher selectivity (SI > 101.26) than 8b (SI = 91.64). Furthermore, compound 8a proved to be more potent than compound 8d, carrying a less

Table 3. In Vitro Antileishmanial Activity of Quinazolinone–Peptide (9a–i)



Entry	R ₁	R ₂	Anti-promastigote activity IC ₅₀ (μM)	Anti-amastigote activity IC ₅₀ ^a (μM)	Cytotoxicity ^b CC ₅₀ (μM) on J-774A.1 cell line	Cytotoxicity CC ₅₀ (μM) on vero cell line	Selectivity Index ^c (SI)
9a			>40	12.03 ± 1.4	>400	>400	>33.25
9b			>40	29.60 ± 3.6	ND ^d	ND	NA ^e
9c			>40	13.48 ± 1.8	>400	>400	>29.67
9d			>40	15.59 ± 1.7	ND	ND	NA
9e			9.34 ± 1.5	14.18 ± 1.0	>400	>400	>28.20
9f			>40	0.73 ± 0.2	>400	>400	>547.94
9g			>40	4.74 ± 0.9	>400	>400	>84.38
9h			>40	15.49 ± 2.1	ND	ND	NA
9i			39.53 ± 3.6	15.79 ± 1.8	ND	ND	NA

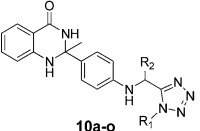
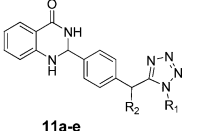
^aIC₅₀ values are the average of two independent assays expressed as average ± standard error. ^bCC₅₀ on J-774A.1 cells. ^cThe selectivity index (SI) is defined as the ratio of (^b) to IC₅₀ on *L. donovani* intracellular amastigotes (^a). ^dND: not determined. ^eNA: not available.

basic morpholine. In addition, tetrahydroisoquinoline containing analogue **8g** exhibited potent antiamastigote activity (IC₅₀ = 4.39 ± 1.4 μM) and high selectivity (SI > 91.11), whereas the tetrahydroquinoline containing analogue **8f** was inactive, indicating that the position of nitrogen atom on the tetrahydro ring is critical in antiamastigote activity. Compound **8h**, having an amyl amine substituent, demonstrated the best potency among all the synthesized quinazolinone–triazine analogues, with IC₅₀ value of 2.42 ± 0.9 μM without any cytotoxicity toward both J-774A.1 and Vero cells (CC₅₀ > 400 μM). Moreover, compound **8h** has a very high selective index (SI > 165.29). Considering the importance of alkyl amine, we have synthesized *n*-butyl and *n*-propyl substituted derivatives **8i** and **8j** for SAR, which were found to be less potent than **8h** with IC₅₀ = 4.80 ± 1.1 μM and IC₅₀ = 8.87 ± 2.1 μM respectively. On the other side, *tert*-butyl substituted derivative **8k** exhibited comparable activity (IC₅₀ = 5.48 ± 1.7 μM) and selectivity with the *n*-butyl containing analogue **8i**. Surprisingly, all the aminoalkyl substituted analogues did not cause toxic effects to Vero cells (CC₅₀ from 141.59 ± 7.4 to >400 μM). Our SAR studies indicated that aminoalkyl substituent is required for good antileishmanial activity of the quinazolinone–triazine hybrid. Introduction of a benzyl group into the quinazolinone–triazine generated a compound (**8n**) with good antiamastigote activity

(IC₅₀ = 6.72 ± 1.1 μM) without any toxic effect to Vero cells (CC₅₀ value of 359.25 ± 12.5 μM) and J-774A.1 cells (CC₅₀ > 400 μM) and has a significant selectivity index (SI > 59.52). However, polar methoxy group carrying benzyl functionality lost the antiamastigote activity of compound **8o**.

In Vitro Antileishmanial Activity of Quinazolinone–Peptide. The encouraging results of the above series prompted us to carry out further structural optimization with the quinazolinone skeleton. Therefore, quinazolinone–peptides (**9a–i**, Scheme 3) via Ugi multicomponent reaction, offer advantages and flexibility to access the desired hybrid for further SAR. The *tert*-butyl isocyanide and cyclohexyl isocyanide were chosen as a model input for this reaction. Synthesized hybrids that were found to be inactive against promastigote nevertheless showed poor to excellent antiamastigote activity, which was demonstrated in Table 3. Compounds **9a** and **9c** exhibited poor antiamastigote activity (*p*-isopropylarylidine, IC₅₀ 12.03 ± 1.4 μM; *p*-chloroarylidine, IC₅₀ 13.48 ± 1.8 μM) but did not show any toxicity. Compounds **9b** and **9d**, which contained the *p*-methoxy and *p*-bromo arylidinesubstituents with *tert*-butylisocyanide functionality, were inactive. Considering the importance of ferrocene-containing heterocycles in organometallic synthesis and in medicinal chemistry,⁵⁴ we have introduced the ferrocene functionality in the quinazolinone skeleton via Ugi multi-

Table 4. In Vitro Antileishmanial Activity of Quinazolinone–Tetrazole (10a–o)

		 10a–o		 11a–e			
Entry	R ₁	R ₂	Anti-promastigote activity IC ₅₀ (μM)	Anti-amastigote activity IC ₅₀ ^a (μM)	Cytotoxicity ^b CC ₅₀ (μM) on J-774A.1 cell line	Cytotoxicity CC ₅₀ (μM) on vero cell line	Selectivity Index ^c (SI)
10a			4.02 ± 1.2	7.76 ± 2.1	>400	>400	>51.54
10b			3.05 ± 1.2	13.05 ± 1.6	>400	>400	>30.65
10c			>40	>40	ND ^d	ND	NA ^e
10d			3.68 ± 1.2	>20	ND	ND	NA
10e			1.21 ± 0.2	7.06 ± 1.4	>400	>400	>56.65
10f			24.06 ± 2.4	8.46 ± 1.7	399.98 ± 15.8	>400	47.28
10g			>40	>40	ND	ND	NA
10h			3.92 ± 1.1	>20	ND	ND	NA
10i			2.56 ± 0.8	15.53 ± 3.1	ND	ND	NA
10j			32.76 ± 2.8	>40	ND	ND	NA
10k			7.00 ± 2.5	9.07 ± 1.2	>400	>400	>44.10
10l			>40	16.76 ± 2.6	ND	ND	NA
10m			39.42 ± 4.5	11.33 ± 1.2	>400	>400	>35.30
10n			>40	9.42 ± 0.8	>400	>400	>42.46
10o			35.95 ± 2.1	19.61 ± 2.0	ND	ND	NA
11a			3.64 ± 1.2	>40	ND	ND	NA
11b			1.91 ± 1.2	>40	ND	ND	NA
11c			5.59 ± 2.0	>40	ND	ND	NA
11d			1.27 ± 0.6	>40	ND	ND	NA
11e			NT	NT	NT	NT	NT
Miltefosine ^f			1.05 ± 0.2	8.4 ± 2.1	12.42 ± 3.2	52.47 ± 2.4	1.48
SSG			947 ± 8.5	46.70 ± 2.8	297.38 ± 10.2	>400	>6.36

^aIC₅₀ values are the average of two independent assays expressed as average ± standard error. ^bCC₅₀ on J-774A.1 cells. ^cThe selectivity index (SI) is defined as the ratio of CC₅₀ on J-774A.1 cells (^b) to IC₅₀ on *L. donovani* intracellular amastigotes (^a). ^dND: not determined. ^eNA: not available. NT: not tested ^f SSG: sodium stibogluconate.

component reaction (9e; *tert*-butyl as R₁) showed moderate activity (IC₅₀ = 14.18 ± 1.0 μM). To evaluate the effect of

cyclohexyl over *tert*-butyl, we synthesized the quinazolinone–peptide 9f. To our surprise, hybrid 9f showed an excellent

antileishmanial activity with IC_{50} value of $0.73 \pm 0.2 \mu M$, which is 12-fold more potent than miltefosine. However, both the ferrocene analogues (**9e** and **9f**) were found to be nontoxic to both J-774A.1 and Vero cells ($CC_{50} > 400 \mu M$). Compound **9f** showed the best selectivity, as indicated by the high value of selective index ($SI > 547.93$, Table 3) and was found to be the most promising in vitro among all the synthesized analogues. SAR was achieved through the combination of a quinazolinone with a metal (Fe) containing fragment; such a hybrid can translate into an enhanced activity of **9f** with high selectivity compared to the other analogues. Introducing the isopropyl in the *p*-position of aryl part and *tert*-butyl as the R_1 group (compound **9a**) exhibited the moderate activity with $IC_{50} = 12.03 \pm 1.4 \mu M$. While the replacement of the *tert*-butyl with cyclohexyl as the R_1 group with the same aromatic ring, i.e., *p*-isopropyl arylidene (compound **9g**; $IC_{50} = 4.74 \pm 0.9 \mu M$), led to 3-fold enhancement of the leishmanicidal activity as compared to **9a**, it displayed no toxicity toward J-774A.1 and Vero cells ($CC_{50} > 400 \mu M$). Interestingly, compounds **9f** and **9g** were more potent than the natural product (Almiramide A–C). On the contrary, *p*-methoxy and *p*-chloro arylidene as the R_2 and cyclohexyl as the R_1 group substituted analogues **9h** and **9i** did not show any antileishmanial activity.

In Vitro Antileishmanial Activity of Quinazolinone–Tetrazole. To find out the role of the effect of Ugi products in the form of tetrazole scaffolds, we have synthesized the quinazolinone–tetrazole hybrid (**10a–o**, **11a–e**, Schemes 3 and 4) and screened for their in vitro antileishmanial activity (Table 4). Compounds **10a**, **10e**, **10f**, **10h**, **10i**, and **10k** exhibited significant antipromastigote activity with IC_{50} value in the range of 1.21 ± 0.2 to $7.00 \pm 2.5 \mu M$, whereas compounds **10a**, **10e**, **10f**, and **10k** exhibited good antiamastigote activity against the pathogen *L. donovani* with IC_{50} values in the range of 7.06 ± 1.4 to $9.07 \pm 1.2 \mu M$ (Table 4). The quinazolinone–tetrazole hybrid **10a**, having *p*-isopropyl substituent on the aryl ring, displayed good antileishmanial activity ($IC_{50} = 7.76 \pm 2.1 \mu M$), while compound **10k** with cyclohexyl instead of *tert*-butyl displayed weak activity ($IC_{50} = 9.07 \pm 1.2 \mu M$). Interestingly, both the derivatives (**10a** and **10k**) were nontoxic to J-774A.1 and Vero cells ($CC_{50} > 400 \mu M$). Compounds **10e** and **10f**, which contain halo substituents such as chloro and bromo on aryl ring, displayed comparable activity ($IC_{50} = 7.06 \pm 1.4 \mu M$ and $IC_{50} = 8.46 \pm 1.7 \mu M$, respectively) without any toxicity. Modification of R_1 from *tert*-butyl to cyclohexyl in the analogues **10m** and **10n**, having *p*-chloro and *p*-bromo arylidene substituents, exhibited less potency with IC_{50} value of $11.33 \pm 1.2 \mu M$ and $9.42 \pm 0.8 \mu M$, respectively, than the compounds **10e** and **10f**. However, *p*-fluoro aryl substituted analogue **10d** was inactive. *tert*-Butyl as the R_1 group and a moderate electron releasing group such as mono methoxyarylidene containing analogue **10b** showed poor leishmanicidal activity ($IC_{50} = 13.05 \pm 1.6 \mu M$), whereas trimethoxy arylidene substituted analogue **10c** displayed no inhibition. These results indicated that *tert*-butyl as R_1 functionality containing hybrids have a pivotal role in antileishmanial activity than the cyclohexyl carrying one. Introduction of heterocyclic moiety like pyridine as a part of R_2 in the compound **10g** resulted in a complete loss of activity. For the sterical demand of the aryl portion, we introduced the naphthyl and 4-methoxynaphthyl as the R_2 and *tert*-butyl as the R_1 group (compounds **10h** and **10i**), did not show antiamastigote activity, which is likely to be due to its steric properties. To our surprise, compounds **10j** and **10o** bearing the ferrocene fragment as a part of R_2 and *tert*-butyl as R_1 were found

to be inactive. Interestingly, compounds **10a**, **10b**, **10e**, **10k**, **10m**, and **10n** was nontoxic to J-774A.1 and Vero cells ($CC_{50} > 400 \mu M$) with good selectivity (SI ranging from >30.65 to 56.65). On the other side, another series of quinazolinone–tetrazole hybrids (**11a–e**) was found to be inactive against the amastigote stages of the parasite. However, compounds **11a–d** demonstrated moderate antipromastigote activity with IC_{50} value in the range of 1.27 ± 0.6 to $5.59 \pm 2.05 \mu M$.

The compounds that combine with high leishmanicidal activity and low or no cytotoxicity were **5b**, **5c**, **5f**, **5g**, **8a**, **8b**, **8g–k**, **8n**, **9a**, **9c**, **9f**, **9g**, **10a**, **10b**, **10e**, **10f**, **10k**, **10m**, and **10n**. Moreover, these analogues exhibited high selectivity as indicated by the high value of selective index (SI ranging from 22.41 to >547.94), which was several-fold better than miltefosine ($SI = 1.48$) and SSG ($SI > 8.57$).

The higher potency of quinazolinone analogues against the amastigote stage of the parasite may be due to the activation of murine macrophages to produce microbicidal molecules and represent a new lead in the development of antileishmanial drugs.

Calculated physicochemical properties of the most potent antileishmanial compounds were done (Table 5) using

Table 5. Calculated Physical Properties of Best Active Antileishmanial Compounds

entry	acceptable range	MW (g/mol) <500	log $P < 5$	nrothb	no. Lipinski violations
5f		427.8	4.49	3	0
8a		498.6	6.23	5	1
8g		594.7	7.19	5	2
8h		502.6	7.57	13	2
8n		542.6	6.49	9	2
9f		715.0	5.77	9	2
9g		649.2	8.53	8	2
10a		509.2	6.03	7	2
miltefosine		407.56	−0.21	20	0

moleinspiration to assess if they were compliant with the Lipinski “rule of five” criteria (Table 5); the data showed that all molecules have (a) molecular weight in the range of 427–715 g/mol, which is lower and higher than the accepted 500 g/mol, and (b) log P close or higher to 5.0, which may indicate that the compounds are too much lipophilic. The compounds **5f** and **8a** did not show violation of the above criteria (Table 5), which exhibited the good in vitro activity (Table 1 and 2). Although the other most active compounds **8g**, **8h**, **8n**, **9f**, **9g**, and **10a** did not meet the compliance to the Lipinski rule of five. Therefore, obtained results of this informative analysis do not counsel that any of the ligands should be discarded from this computational assessment and they should be taken in account for further lead optimization.

Production of Host Protective Cytokines in Murine Macrophages Induced by Compounds **8a and **8g**.** Leishmania prevents the activation of an effective immune response by repression of a number of pro-inflammatory cytokines that included IL-1, IL-12, and TNF- α . For the effective clearance of parasite burden, it is necessary to augment host immune responses by the production of these protective cytokines. Th1 type cytokines, IL-12, and TNF- α play a critical role in the repression of immunosuppressive cytokines IL-10 and TGF- β . Our results indicate that quinazolinone–triazine analogues, **8a** and **8g**, induce the activation of IL-12 and TNF- α in treated murine macrophage cells and mediate effective

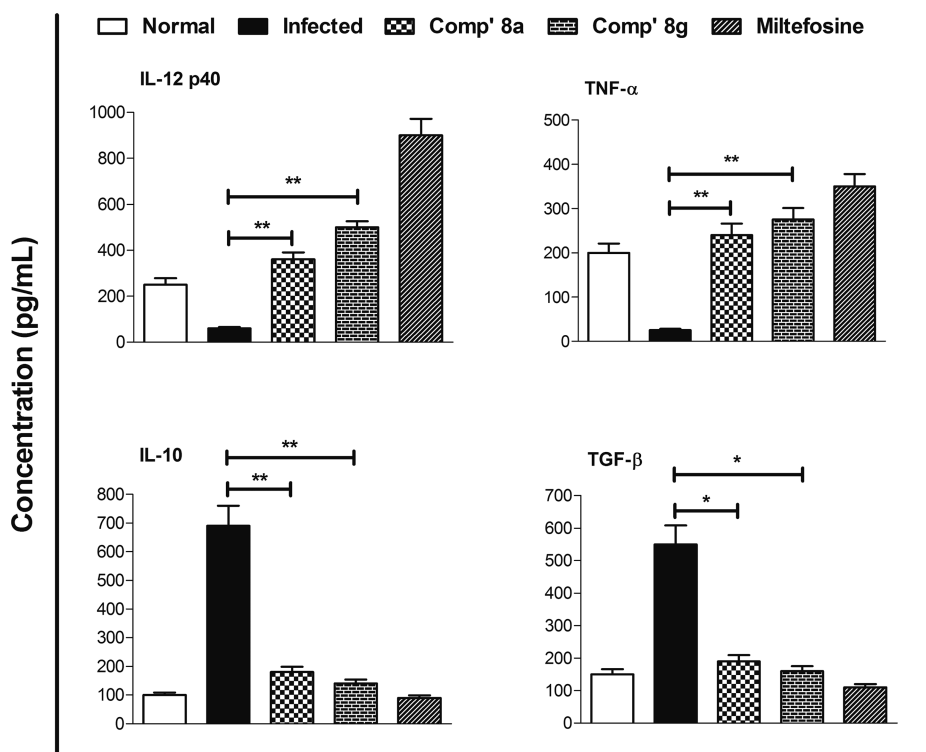


Figure 7. Compounds **8a** and **8g** mediated antileishmanial activity via up-regulation of Th1 cytokines (IL-12 and TNF- α) and down-regulation of Th2 cytokines (IL-10 and TGF- β) in infected murine macrophage (J774-A.1) cell line. The levels of cytokine release (pg/mL) in the culture supernatant were evaluated by sandwich ELISA after 24 h post treatment. Results were expressed as mean \pm SD from two independent experiments. The asterisks indicate statistically significant increase and decrease (*, $p < 0.05$; **, $p < 0.01$; ***, $p < 0.001$) in cytokine production compared between infected macrophages versus **8a** treated and infected versus **8g** treated macrophages. Miltefosine was used as a reference drug.

suppression of parasite multiplication by abrogation of *L. donovani* induced anti-inflammatory cytokines, IL-10 and TGF- β . A comparative cytokine profile of compound **8g** treated leishmania-infected cells showed >8- and 11-fold ($p < 0.01$) increase in IL-12 and TNF- α production, respectively. On the other hand, **8g** treated cells showed ~5- ($p < 0.01$) and >3-fold ($p < 0.05$) decrease in IL-10 and TGF- β production, respectively, in comparison with untreated infected cells. Moreover, **8a** treated cells also showed 6- and >9-fold ($p < 0.01$) increase in IL-12 and TNF- α and >3- ($p < 0.01$) and 2.8-fold ($p < 0.05$) decrease in IL-10 and TGF- β production, respectively (Figure 7).

Induction of Nitric Oxide Generation in Murine Macrophages in Vitro by Compounds 8a and 8g. Along with pro-inflammatory cytokines, production of deadly microbicidal agent nitric oxide (NO) by macrophages play a crucial role in intracellular parasite killing by oxidative stress. IL-10 and TGF- β inhibit the expression of inducible nitric oxide synthase (iNOS), responsible for NO generation. Compounds **8a** and **8g** treated leishmania-infected macrophages stimulated murine macrophages and produced significant amount of nitrite, 15.72 and 22.58 μ M, respectively, which was >3- ($p < 0.01$) and ~5-fold ($p < 0.05$) higher than infected untreated cells (4.65 μ M) (Figure 8). Thus, significant generation of nitrite by compounds **8a** and **8g** treated cells promotes elimination of *L. donovani* parasites (Figure 8).

In Vivo Activity against *L. donovani*/Hamster Model. Because of the highly promising results obtained for this novel family of quinazolinone hybrids (**5e**, **8a**, **8b**, **8g**, **8h**, **8n**, **9f**, **9i**, and **10a**) in our in vitro studies, they appeared as excellent candidates for further drug development; to that end, in vivo tests were performed in the golden hamster model. The aqueous

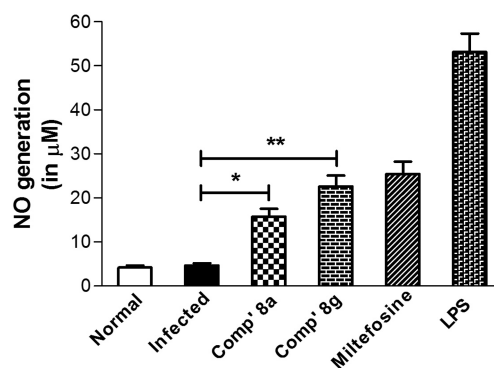


Figure 8. Nitric oxide production (μ M) by infected murine macrophage J-774 cells in response to **8a**, **8g**, and miltefosine at IC₅₀ dose. The absorbance of the reaction product was measured at 540 nm using Griess reagent. The asterisks indicate statistically significant induction (*, $p < 0.05$; **, $p < 0.01$; ***, $p < 0.001$) of NO production compared between infected versus **8a** treated and infected versus **8g** treated J774 cells. Miltefosine was used as a reference drug, and lipopolysaccharide (LPS 10 μ g/mL) was used as a mitogen.

suspensions of tested compounds were administered for five consecutive days at 50 mg/kg/day by IP route. The post-treatment splenic biopsies were done on day 7 of the last dose administration, and amastigote counts were assessed by Giemsa staining (Table 5). Compound **5e** showed poor percentage inhibition of 35.83 ± 10.6 . Compounds **8a** and **8g** showed the best in vivo efficacy among the all tested analogues, on average 73.15 ± 12.69 and $80.93 \pm 10.50\%$ inhibitions, respectively, in parasite multiplication. In contrast, compounds **8h** and **8n** have shown moderate inhibition of 43.01 ± 10.30 and $44.83 \pm$

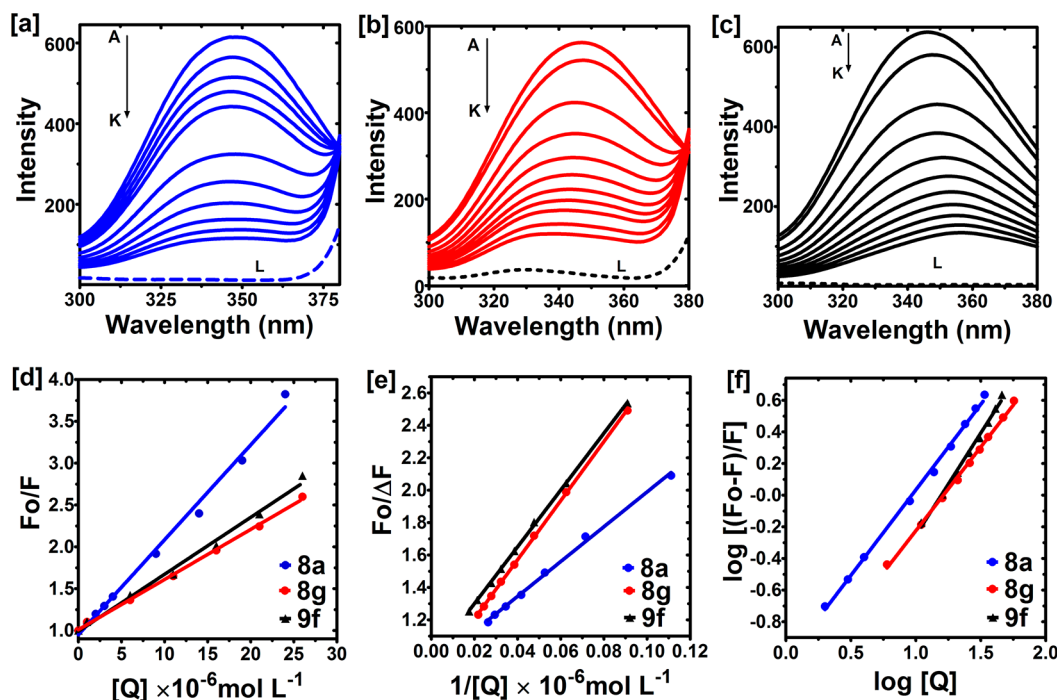


Figure 9. Fluorescence analysis of BSA–compound interaction. (a) Intrinsic fluorescence emission spectra of BSA (1.0×10^{-5} M) excited at 280 nm in the presence of various concentrations (A–L represent 0, 1, 2, 3, 4, 9, 14, 19, 24, 29, 34, and 38 μ M compound, respectively) of compound 8a, and M represents emission spectra of 10 μ M 8a alone excited at 280 nm. (b) Intrinsic fluorescence of BSA in the presence of various concentrations of compound 8g (A–K represents 0, 1, 6, 11, 16, 21, 26, 31, 36, 47, and 57 μ M compound respectively), and L represents emission fluorescence of 10 μ M 8g alone). (c) Intrinsic fluorescence spectra of BSA in the presence of various concentrations of compound 9f (A–K represents 0, 1, 6, 11, 16, 21, 26, 31, 36, 41, and 46 μ M of 9f, respectively), and L represents emission spectra of 10 μ M 9f alone excited at 280 nm. (d) Stern–Volmer plots for quenching of BSA by compounds. (e) Modified Stern–Volmer plots for quenching of BSA by compounds. (f) Plots of $\log [(F_0 - F)/F]$ versus $\log [Q]$.

Table 7. Binding Parameters and Site of Compound–BSA Interaction at pH 7.4^a

Entry	K_{sv} (L mol ⁻¹)	K_q (L mol ⁻¹ s ⁻¹)	R^a	K_a (L mol ⁻¹)	R^b	N	R^c
8a	10.0×10^4	10×10^{12}	0.9983	7.9×10^4	0.9988	1.08	0.9980
8g	6.0×10^4	6.0×10^{12}	0.9970	5.8×10^4	0.9992	1.05	0.9980
9f	7.0×10^4	7.0×10^{12}	0.9962	4.6×10^4	0.9998	1.2	0.9946

^a R^a , R^b , and R^c are correlation coefficients for Stern–Volmer plots, modified Stern–Volmer plots, and plots of log analysis of fluorescence, respectively.

12.26%, respectively. Quinazolinone–peptide (9f) displayed better in vivo inhibition of $51.42 \pm 15.67\%$ than 9i (48.05 ± 13.60), whereas quinazolinone–tetrazole hybrid 10a exhibited above moderate inhibition of $54.01 \pm 10.65\%$.

Intrinsic Fluorescence Quenching. To find out the binding parameters, mechanism of quenching and mode of interaction of most active compounds 8a, 8g, and 9f with BSA, fluorescence spectroscopy, and UV–vis absorption spectroscopy were performed. Fluorescence quenching is useful in finding the binding behavior of small molecules with proteins. BSA showed characteristic emission peak at 343 nm upon excitation at 280 nm. Fluorescence intensity was decreased gradually with increasing concentration of compounds as shown in Figure 9a–c. All three compounds showed fluorescence quenching and shift in fluorescence (345 to 359 nm with 8a, 345 to 336 nm with 8g, and 345 to 356 nm with 9f) of BSA. All the compounds showed strong protein binding, and extent of protein binding was similar for all compounds studied. The decrease in fluorescence intensity is usually described by the Stern–Volmer equation:⁵⁵

$$F_0/F = 1 + K_{SV}[Q] = 1 + K_q\tau_0[Q]$$

where F_0 and F are the fluorescence intensities before and after the addition of the compound or quencher, respectively, K_{SV} is the dynamic quenching constant; K_q is the quenching rate constant; $[Q]$ is the concentration of compound added; τ_0 is the average lifetime of the molecule without quencher and its value is considered to be 10^{-8} s.⁵⁶

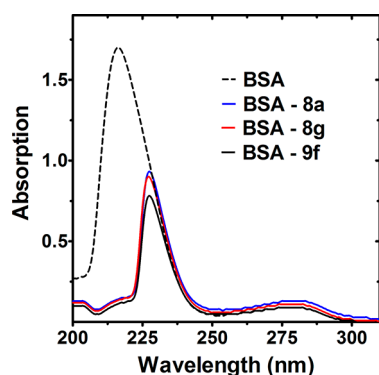
Stern–Volmer plots for compounds showed good linear relationship with the increasing concentrations (Figure 9d). The results showed that higher values of K_q (Table 7) than the maximum value of the scattering collision quenching constant (2.0×10^{10} L mol⁻¹ s⁻¹) for biomolecules,⁵⁷ indicating the probable quenching mechanism of BSA–compound interactions was initiated by complex formation.

To confirm that quenching of BSA fluorescence by compounds is due to static complex formation, the difference absorption spectroscopy was employed. The UV–vis absorption spectrum of BSA and the difference absorption spectrum between BSA–compound complex and compound alone at the same concentration could not be superposed (Figure 10), demonstrating that BSA formed ground state complex with compounds. BSA absorption spectra showed two peaks and change in peak near 210 nm is due to change in conformation in

Table 6. In Vivo Evaluation of Compounds against *L. donovani*/Hamster Model

entry	% inhibition \pm SD (dose = 50 mg/kg \times 5 days, IP route)
Sf	35.83 \pm 10.66
8a	73.15 \pm 12.69
8b	37.43 \pm 08.59
8g	80.93 \pm 10.50
8h	43.01 \pm 10.30
8n	44.83 \pm 12.26
9f	51.42 \pm 15.67
9g	48.05 \pm 13.60
10a	54.01 \pm 10.65
Miltefosine ^a	98.1 \pm 1.2
SSG ^b	86.89 \pm 5.45

^aMiltefosine (30 mg/kg \times 5 days, oral). ^bSSG, sodium stibogluconate (40 mg/kg \times 5 days, IP) used as reference drugs; SD, standard deviation; IP, intraperitoneal.

**Figure 10.** UV-vis absorption spectra of 1.0×10^{-5} M BSA in the presence of compounds at the 1:1 concentration ratio.

peptide backbone associated with helix coil transformation. The change in microenvironment of tryptophan and tyrosine residues is shown by change in 280 nm peak.⁵⁸ Absorption spectra of BSA (Figure 10) showed that ground state complex formation with compounds is associated with alteration in the conformation of BSA.

Binding Constant and Site. For static quenching of BSA fluorescence data were analyzed by Modified Stern–Volmer⁵⁹ equation:

$$F_0/\Delta F = \{1/(f_a K_a [Q])\} + 1/f_a$$

ΔF is the difference of fluorescence in the absence and presence of compounds at concentration $[Q]$, f_a is the fraction of accessible fluorescence, and K_a is the effective quenching constant for the accessible fluorophores, which is similar to the binding constant for the quencher–acceptor systems. The dependence of $F_0/\Delta F$ on the reciprocal value of concentration $[Q]^{-1}$ is linear, with the slope equaling to the value of $(f_a K_a)^{-1}$. The modified Stern–Volmer plots were demonstrated in Figure 9e.

In static quenching, the equilibrium between free and bound molecules can be given by the equation:⁶⁰

$$\log(F_0 - F)/F = \log K_A + n \log [Q]$$

K_A and n are binding constant and number of binding sites, respectively.

The double logarithm plot has been shown in Figure 9f, and the calculated binding sites (n) are shown in Table 7. The results showed that the values of the binding sites n were approximately 1, indicating the formation of ground state complex is due to single high affinity binding site on protein.

Pharmacokinetics Studies. The pharmacokinetic studies revealed that the animals tolerated the treatment as no peculiarities in the animals' behavior were observed. Calculations of the pharmacokinetic data were based on the mean serum concentrations and were performed by use of the compartmental and noncompartmental approaches using WinNonlin (version 5.1) software. In a comparative pharmacokinetic study, both of the compounds were rapidly absorbed with C_{max} between 1 and 2 after oral dose (Figure 11). A one-compartment open model best described serum concentration–time data of 8a, with elimination from central compartment and a large volume of distribution (3.22 L/kg). Oral serum concentrations were significantly lower than those observed by the intravenous administration as the extent of absolute bioavailability of 8a following oral administration was 5.75% (Table 8). The serum concentration of 8a after intravenous administration decreased biexponentially with the terminal half-life ($t_{1/2\beta}$) of 0.28 h, but its elimination from the central compartment was higher ($t_{1/2k10}$, 0.84 h).

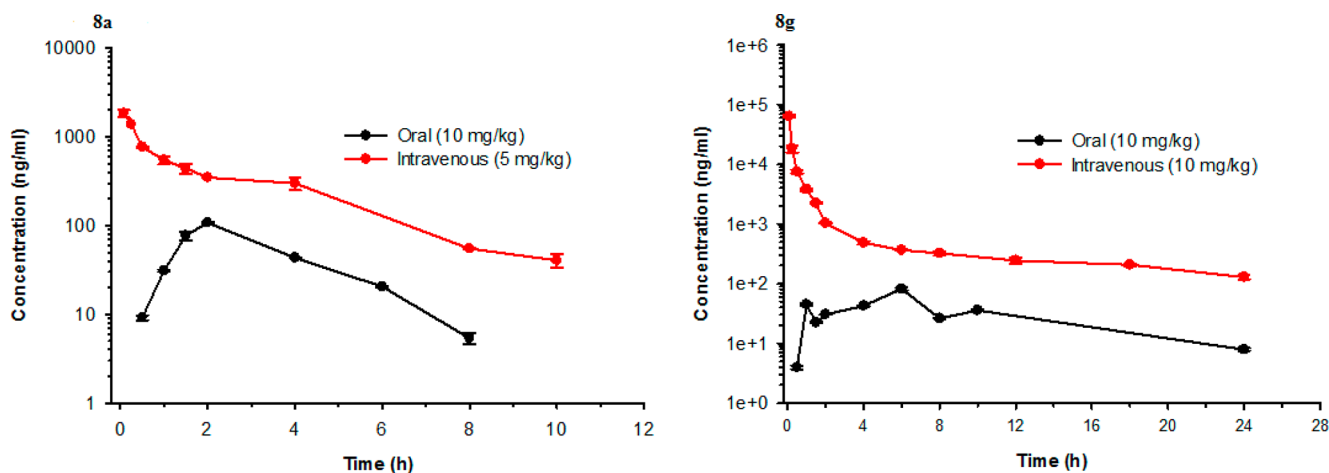
**Figure 11.** Concentration–time profile of compounds 8a and 8g after oral and intravenous administration in male Sprague–Dawley rats. Bar represents SEM.

Table 8. Pharmacokinetic Parameters of Compounds (8a and 8g) after Oral and Intravenous Dose in Male Sprague–Dawley Rats^a

parameters		8a		8g	
		oral	intravenous	oral	intravenous
C_{\max} (ng/mL)	1	107.83 \pm 1.39	1829.48 \pm 172.93	44.72 \pm 1.87	63276.38 \pm 3152.55
	2			81.66 \pm 4.22	
t_{\max} (h)	1	2	0.08	1	0.08
	2			6	
AUC_{0-t} (ng h/mL)		327	2843	716	24341
$t_{1/2}$ (h)		1.26	0.84		12.79
MRT (h)		3.01	3.07	8.44	5.88
V_{ss} (L/kg)		5.39	5.44		1.95
clearance (L/h/kg)		1.79	1.77	0.36	0.33
bioavailability (%)		5.75		2.94	

^aValues of C_{\max} are mean \pm SEM, and the value represents the average of three rats post dose. AUC_{0-t} : area under the serum concentration–time curve up to last sampling time. C_{\max} : serum peak concentration. MRT: mean residence time. t_{\max} : time to C_{\max} . $t_{1/2}$: elimination half-life. V_{ss} : volume of distribution at steady-state.

Following oral administration, **8g** gave two C_{\max} and, therefore, model-independent pharmacokinetic parameters were calculated. The AUC_{0-t} and MRT were 2.2- and 2.8-fold higher and clearance was 5-fold lower than those of **8a** after a single oral dose of 10 mg/kg in rats (Table 8). However, a three-compartmental open model fitted the raw data of **8g** better after intravenous administration than a two-compartmental model based on the observed fit, the residual sum of squared error, the correlation, and the Akaike's Information Criterion.⁶¹ Using an open three-compartment model, the terminal half-life ($t_{1/2\gamma}$) of **8g** was 12.79 h. The AUC_{0-t} was 4-fold higher whereas the serum clearance was 5-fold lower than that of **8a**, although **8a** showed comparatively higher bioavailability but the extent of absorption (AUC_{0-t}), indicating systemic availability and elimination half-life were lower than that of **8g**. However, the systemic clearances of both the compounds were smaller than the hepatic blood flow of the rat (2.9 L/h/kg),⁶² suggesting an insignificant amount of extrahepatic elimination.

CONCLUSION

Four novel series of quinazolinone hybrids bearing interesting bioactive scaffolds (pyrimidine, triazine, tetrazole, and peptide) were synthesized. A number of such compounds exhibited better potency against the intracellular amastigote of *L. donovani* than the standard drugs and were not found to be cytotoxic. The SAR analysis revealed that among the synthesized quinazolinone hybrids, quinazolinone–pyrimidine, triazine, and ferrocene-containing quinazolinone–peptide displayed potent antileishmanial activity. Compounds **8a**, **8g**, and **9f** showed very consistent and promising leishmanicidal activity against intracellular amastigotes and in vivo efficacy in the golden hamster model and displayed no toxicity for macrophages and Vero cells. Furthermore, our data suggest that interaction of most potent compounds **8a**, **8g**, and **9f** with blood proteins showed static and dynamic quenching of intrinsic fluorescence. The data obtained for albumin interaction and pharmacokinetic studies provide information about mode of transport in blood, absorption, distribution, and bioavailability of quinazolinone derivatives. Therefore, these analogues are good candidates for a lead optimization for identifying new analogues to curb the unnecessary loss of life globally.

EXPERIMENTAL SECTION

General. All reagents were commercial and were used without further purification. Chromatography was carried on silica gel (60–120 and 100–200 mesh). All reactions were monitored by thin-layer chromatography (TLC), and silica gel plates with fluorescence F254 were used. Melting points were taken in open capillaries on a Complab melting point apparatus and are presented uncorrected. Infrared spectra were recorded on a Perkin-Elmer AC-1 spectrometer. ¹H NMR and ¹³C NMR spectra were recorded using a BrukerSupercon Magnet DRX-300 spectrometer (operating at 300 MHz for ¹H and 50 and 75 MHz for ¹³C) using CDCl₃ as solvent and tetramethylsilane (TMS) as internal standard. Chemical shifts are reported in parts per million. Multiplicities are reported as follows: singlet (s), doublet (d), triplet (t), multiplet (m), and broad singlet (brs). Some signals for NH proton are not present in the few ¹H NMR data. Electrospray ionization mass spectra (ESIMS) were recorded on Thermo Lcq Advantage Max-IT. High resolution mass spectra (HRMS) were recorded on 6520 Agilent Q TOF LC MS/MS (accurate mass). Purity of final compounds was determined by analytical HPLC, which was carried out on a Waters HPLC system (model pump, 515; detector, PDA-2998). HPLC analysis conditions: Waters Sunfire C18 (5.0 μ M), 4.6 mm \times 250 mm column, flow rate 0.5 mL/min, UV detection at 254 nm. All biologically evaluated compounds are >95% pure.

Representative Procedure for the Synthesis of 2-(4-(3-Oxo-3-phenylprop-1-enyl)phenyl)-2,3-dihydroquinazolin-4(1H)-one (4a). To a stirred solution of **3** (500 mg, 1.98 mmol) and acetophenone (0.23 mL, 1.92 mmol) in ethanol (5 mL) was added KOH as a catalyst. The whole reaction mixture was stirred for 5 h at rt. The obtained precipitate was filtered and washed with water and recrystallized with ethanol to obtain **4a** as a cream solid (550 mg, yield 78%). ¹H NMR (300 MHz, DMSO-*d*₆) δ 8.43 (brs, 1H), 8.21 (d, *J* = 7.26 Hz, 2H), 7.97 (d, *J* = 7.26 Hz, 3H), 7.76 (s, 1H), 7.73–7.61 (m, 1H), 7.65 (t, *J* = 7.77 Hz, 4H), 7.33–7.28 (m, 1H), 7.25 (s, 1H), 7.18 (s, 1H), 6.83 (d, *J* = 8.07 Hz, 1H), 6.76 (t, *J* = 7.53 Hz, 1H) 5.86 (s, 1H). IR (KBr): 3436, 2943, 1634, 1425, 1216 cm⁻¹. ESI-MS C₂₃H₁₈N₂O₂ (*m/z*): 355.0 (*M*⁺ + H).

Synthesis of Other Quinazolinone–Chalcone Hybrid 4b–i. The above procedure was followed for **4b–i**.

2-(4-(3-(3,4,5-Trimethoxyphenyl)acryloyl)phenyl)-2,3-dihydroquinazolin-4(1H)-one (4b). Light-yellow solids (yield 72%). ¹H NMR (300 MHz, DMSO-*d*₆) δ 8.38 (brs, 1H), 7.87 (d, *J* = 7.87 Hz, 2H), 7.69 (s, 1H), 7.69–7.51 (m, 4H), 7.27–7.19 (m, 2H), 7.09 (d, *J* = 8.38 Hz, 1H), 6.70 (d, *J* = 8.12 Hz, 1H), 6.65 (t, *J* = 7.39 Hz, 1H), 5.80 (s, 1H), 3.87 (s, 6H), 3.71 (s, 3H). IR (KBr): 3439, 2926, 1652, 1427, 1218, 780 cm⁻¹. ESI-MS C₂₆H₂₄N₂O₅ (*m/z*): 445 (*M*⁺ + H).

2-(4-(2,3-Dimethoxystyryl)phenyl)-2,3-dihydroquinazolin-4(1H)-one (4c). Light-yellow solids (yield 75%). ¹H NMR (300 MHz, DMSO-*d*₆) δ 8.41 (brs, 1H), 7.92 (d, *J* = 7.92 Hz, 2H), 7.72 (s, 1H), 7.63–7.54 (m, 5H), 7.32–7.22 (m, 2H), 7.12 (d, *J* = 8.40 Hz, 1H), 6.78 (d, *J* = 8.04 Hz, 1H), 6.71 (t, *J* = 7.41 Hz, 1H), 5.80 (s, 1H), 3.87 (s, 6H). IR (KBr):

3424, 2928, 1648, 1418, 1219, 785 cm^{-1} . ESI-MS $\text{C}_{24}\text{H}_{22}\text{N}_2\text{O}_3$ (m/z): 387 ($\text{M}^+ + \text{H}$).

2-(4-(4-Methoxystyryl)phenyl)-2,3-dihydroquinazolin-4(1H)-one (4d). Cream solid (yield 72%). ^1H NMR (300 MHz, $\text{DMSO}-d_6$) δ 8.34 (brs, 1H), 8.17 (d, $J = 8.64$ Hz, 2H), 7.96–7.87 (m, 3H), 7.72–7.54 (m, 4H), 7.28 (t, $J = 7.80$ Hz, 1H), 7.17 (s, 1H), 7.10 (d, $J = 8.64$ Hz, 2H), 6.78 (d, $J = 8.13$ Hz, 1H), 6.71 (t, $J = 7.35$ Hz, 1H), 5.80 (s, 1H), 3.87 (s, 3H). IR (KBr): 3426, 2923, 1620, 1416, 1218, 770 cm^{-1} . ESI-MS $\text{C}_{23}\text{H}_{20}\text{N}_2\text{O}_2$ (m/z): 357 ($\text{M}^+ + \text{H}$).

2-(4-(4-Fluorostyryl)phenyl)-2,3-dihydroquinazolin-4(1H)-one (4e). Cream solid (yield 72%). ^1H NMR (300 MHz, $\text{DMSO}-d_6$) δ 8.07 (brs, 1H), 7.99 (s, 1H), 7.89 (s, 2H), 7.66–7.56 (m, 8H), 7.16 (s, 2H), 6.75–6.63 (m, 2H), 5.76 (s, 1H). IR (KBr): 3435, 2927, 1634, 1423, 1218, 772 cm^{-1} . ESI-MS $\text{C}_{22}\text{H}_{17}\text{FN}_2\text{O}$ (m/z): 345 ($\text{M}^+ + \text{H}$).

2-(4-(4-Chlorostyryl)phenyl)-2,3-dihydroquinazolin-4(1H)-one (4f). Light-yellow solid (yield 70%). ^1H NMR (300 MHz, $\text{DMSO}-d_6$) δ 8.35 (brs, 1H), 8.18 (d, $J = 8.37$ Hz, 2H), 7.92–7.89 (m, 3H), 7.77 (s, 1H), 7.65 (t, $J = 8.10$ Hz, 3H), 7.58 (d, $J = 7.89$ Hz, 2H), 7.28 (t, $J = 7.05$ Hz, 1H), 7.18 (s, 1H), 6.78 (d, $J = 7.95$ Hz, 1H), 6.71 (d, $J = 7.41$ Hz, 1H), 5.81 (s, 1H). IR (KBr): 3436, 2943, 1634, 1425, 1216, 779 cm^{-1} . ESI-MS $\text{C}_{22}\text{H}_{17}\text{ClN}_2\text{O}$ (m/z): 361 ($\text{M}^+ + \text{H}$).

2-(4-(4-Bromostyryl)phenyl)-2,3-dihydroquinazolin-4(1H)-one (4g). Cream solid (yield 69%). ^1H NMR (300 MHz, $\text{DMSO}-d_6$) δ 8.36 (brs, 1H), 8.16 (d, $J = 8.07$ Hz, 2H), 7.94–7.83 (m, 2H), 7.76 (s, 1H), 7.68 (t, $J = 8.10$ Hz, 3H), 7.59 (d, $J = 7.90$ Hz, 2H), 7.25 (t, $J = 7.15$ Hz, 1H), 7.17 (s, 1H), 6.74 (d, $J = 7.92$ Hz, 1H), 6.70 (d, $J = 7.31$ Hz, 1H), 5.83 (s, 1H). IR (KBr): 3436, 2926, 1649, 1411, 1219, 680 cm^{-1} . ESI-MS $\text{C}_{22}\text{H}_{17}\text{BrN}_2\text{O}$ (m/z): 405 ($\text{M}^+ + \text{H}$).

2-(4-(3-(2-Chlorophenyl)acryloyl)phenyl)-2,3-dihydroquinazolin-4(1H)-one (4h). Yellow solid (yield 70%). ^1H NMR (300 MHz, $\text{DMSO}-d_6$) δ 8.42 (brs, 1H), 7.85 (d, $J = 8.19$ Hz, 2H), 7.67–7.57 (m, 7H), 7.43 (s, 1H), 7.36 (s, 1H), 7.31–7.27 (m, 1H), 7.24 (s, 1H), 6.82 (d, $J = 8.04$ Hz, 1H), 6.75 (t, $J = 7.53$ Hz, 1H), 5.84 (s, 1H). IR (KBr): 3436, 2943, 1634, 1425, 1216, 776 cm^{-1} . ESI-MS $\text{C}_{22}\text{H}_{17}\text{ClN}_2\text{O}$ (m/z): 361 ($\text{M}^+ + \text{H}$).

2-(4-(4-(4-Methylpiperazin-1-yl)styryl)phenyl)-2,3-dihydroquinazolin-4(1H)-one (4i). Yellow solid (yield 70%). ^1H NMR (300 MHz, $\text{DMSO}-d_6$) δ 8.34 (brs, 1H), 8.05 (d, $J = 8.64$ Hz, 2H), 7.93 (s, 1H), 7.88 (d, $J = 7.2$ Hz, 2H), 7.71–7.61 (m, 2H), 7.56 (d, $J = 8.04$ Hz, 2H), 7.28 (t, $J = 7.62$ Hz, 1H), 7.16 (s, 1H), 7.03 (d, $J = 8.67$ Hz, 2H), 6.78 (d, $J = 7.95$ Hz, 1H), 6.71 (t, $J = 7.47$ Hz, 1H), 5.79 (s, 1H), 3.33 (brs, 4H), 2.44 (brs, 4H), 2.23 (s, 3H). IR (KBr): 3406, 2932, 1650, 1417, 1220, 770 cm^{-1} . ESI-MS $\text{C}_{27}\text{H}_{28}\text{N}_4\text{O}$ (m/z): 425 ($\text{M}^+ + \text{H}$).

Representative Procedure for the Synthesis of 2-(4-(2-Amino-6-phenylpyrimidin-4-yl)phenyl)-2,3-dihydroquinazolin-4(1H)-one (5a). To a stirred solution of NaH (108 mg, 4.5 mmol) and guanidine hydrochloride (214 mg, 2.25 mmol) in DMF (3 mL) was added gradually 4a (400 mg, 1.12 mmol), and the reaction mixture was stirred for 10 min at rt and then heated at 60 °C for 5 h. After the completion of reaction, the reaction mixture was poured into water and the obtained precipitate was filtered and purified by column chromatography (eluting with 2% methanol in chloroform) to afford the quinazolinone-pyrimidine 5a as light-yellow solid (310 mg, yield 70%); mp 175–177 °C. HPLC-DAD: $t_r = 6.5$ min (% area = 97.2%). ^1H NMR (300 MHz, $\text{DMSO}-d_6$) δ 8.38 (brs, 1H), 8.25–8.23 (m, 4H), 7.72–7.63 (m, 4H), 7.52 (s, 3H), 7.29 (t, $J = 7.02$ Hz, 1H), 7.20 (s, 1H), 6.79–6.76 (m, 3H), 6.72 (t, $J = 7.47$ Hz, 1H), 5.85 (s, 1H). ^{13}C NMR (75 MHz, $\text{DMSO}-d_6$) δ 165.39, 164.85, 164.47, 164.05, 148.28, 144.25, 137.96, 133.83, 130.94, 129.08, 127.84, 117.71, 115.48, 114.94, 102.37, 66.72. IR (KBr): 3411, 3019, 1654, 1569, 1451, 1218, 1063 cm^{-1} . ESI-MS $\text{C}_{24}\text{H}_{19}\text{N}_5\text{O}$ (m/z): 394 ($\text{M}^+ + \text{H}$). HRMS: calcd, 394.1662 (MH^+); found, 394.1666 (MH^+).

Representative Procedure for the Synthesis of 2-(4-Amino-phenyl)-2-methyl-2,3-dihydroquinazolin-4(1H)-one (7). To a stirred solution of anthralinamide (1.0 g, 7.39 mmol) and 4-aminoacetophenone (1.0 g, 7.35 mmol) in methanol (10 mL) were added acidic silica as a catalyst. The reaction mixture was heated at 60 °C for 3 h, and the conversion was monitored by TLC. The reaction mixture was evaporated and formed residue was mixed with water and chloroform and purified by crystallization with acetonitrile to afford 7 as a cream solid (1.6 g, yield 85%). ^1H NMR (300 MHz, $\text{DMSO}-d_6$) δ

8.51 (brs, 1H), 7.49 (d, $J = 7.62$ Hz, 1H), 7.37 (brs, 1H), 7.20–7.10 (m, 3H), 6.72 (d, $J = 8.07$ Hz, 1H), 6.58 (t, $J = 7.35$ Hz, 1H), 6.44 (d, $J = 8.04$ Hz, 2H), 4.95 (brs, 2H). IR (KBr): 3423, 3314, 2932, 1624, 1410, 1224 cm^{-1} . ESI-MS $\text{C}_{15}\text{H}_{15}\text{N}_3\text{O}$ (m/z): 254.0 ($\text{M}^+ + \text{H}$).

Representative Procedure for the Synthesis of 2-(4-(4,6-Di(piperidin-1-yl)-1,3,5-triazin-2-ylamino)phenyl)-2-methyl-2,3-dihydroquinazolin-4(1H)-one (8a). The solution of compound 7 (500 mg, 1.98 mmol) in dry THF was added dropwise to an ice-cold mixture of cyanuric chloride (401 mg, 2.17 mmol) in dry THF. The reaction mixture was stirred at room temperature for 1 h, and then the solvent was removed in vacuo and formed crude product was mixed with K_2CO_3 (550 mg, 3.95 mmol) and piperidine (0.39 mL, 4.58 mmol) in dry DMF. The whole reaction mixture was heated at 70 °C until completion of reaction. On completion of the reaction (checked by TLC analysis), the reaction mixture was poured into ice–water, and obtained precipitate was filtered. The crude product was subjected to silica gel column chromatography using chloroform/methanol as mobile phase (9:1) to afford the desired compound 8a as white solid (700 mg, yield 71%); mp 160–162 °C. HPLC-DAD: $t_r = 9.6$ min (% area = 97.3%). ^1H NMR (300 MHz, $\text{CDCl}_3 + \text{DMSO}-d_6$) δ 7.72 (brs, 1H), 7.56–7.50 (m, 2H), 7.35 (s, 2H), 7.10 (s, 1H), 6.66 (d, $J = 5.4$ Hz, 1H), 6.53 (s, 2H), 3.63 (brs, 8H), 1.69 (s, 3H), 1.55–1.46 (m, 12H). ^{13}C NMR (50 MHz, $\text{CDCl}_3 + \text{DMSO}-d_6$) δ 169.51, 152.35, 145.02, 144.74, 138.26, 132.37, 130.43, 123.58, 121.83, 120.05, 119.47, 75.16, 48.84, 35.62, 35.76, 30.60, 29.65. IR (KBr): 3423, 2934, 2849, 1639, 1574, 1494, 1443, 1370, 1237, 1026 cm^{-1} . ESI-MS $\text{C}_{28}\text{H}_{34}\text{N}_8\text{O}$ (m/z): 499 ($\text{M}^+ + \text{H}$). HRMS: calcd, 499.2928 (MH^+); found, 499.2929 (MH^+).

Representative Procedure for the Synthesis of N-(2-(tert-Butylamino)-1-(4-isopropylphenyl)-2-oxoethyl)-3-chloro-N-(4-(2-methyl-4-oxo-1,2,3,4-tetrahydroquinazolin-2-yl)phenyl)-benzamide (9a). To a stirred solution of 7 (300 mg, 1.18 mmol) in methanol, *m*-chlorobenzoic acid (218 mg, 1.18 mmol), isopropyl benzaldehyde (0.17 mL, 1.37 mmol), and *tert*-butyl isocyanide (0.13 mL, 1.61 mmol) was successively added, and the reaction mixture was stirred at rt for 6 h. After completion of reaction (checked by TLC analysis), the methanol was removed and the residue was purified by silica gel column chromatography (eluting with 2% methanol in chloroform) to afford the target product 9a as white solid (450 mg, yield 61%); mp 162–164 °C. HPLC-DAD: $t_r = 7.6$ min (% area = 97.3%). ^1H NMR (300 MHz, $\text{DMSO}-d_6$) δ 8.53 (brs, 1H), 7.69 (d, $J = 4.1$ Hz, 1H), 7.42 (d, $J = 7.5$ Hz, 1H), 7.36 (s, 1H), 7.18–7.13 (m, 2H), 7.09–7.03 (m, 4H), 6.93 (t, $J = 7.7$ Hz, 5H), 6.67–6.64 (m, 1H), 6.58 (t, $J = 6.9$ Hz, 1H), 6.09 (s, 1H), 2.73–2.64 (m, 1H), 1.42 (s, 3H), 1.18 (s, 9H), 1.08 (d, $J = 5.2$ Hz, 6H). IR (KBr): 3418, 3325, 2967, 1654, 1563, 1490, 1377, 1218, 767 cm^{-1} . ESI-MS $\text{C}_{37}\text{H}_{39}\text{ClN}_4\text{O}_3$ (m/z): 623.0 ($\text{M}^+ + \text{H}$). HRMS: calcd, 623.2783 (MH^+); found, 623.2783 (MH^+); [$\text{M} + \text{H}$] $^+$.

Representative Procedure for the Synthesis of 2-(4-((1-tert-Butyl-1H-tetrazol-5-yl)(4-isopropylphenyl)methylamino)-phenyl)-2-methyl-2,3-dihydroquinazolin-4(1H)-one (10a). Solution of 7 (300 mg, 1.18 mmol), isopropylbenzaldehyde (1.0 equiv, 1.65 mmol), and *tert*-butyl isocyanide (0.13 mL, 1.61 mmol) was stirred in anhydrous methanol (5 mL) at rt for 10 min. Thereafter, trimethylsilyl azide (0.23 mL, 2.03 mmol) was added and the resulting mixture was further stirred for 7 h. On completion of the reaction (checked by TLC analysis), the methanol was removed in vacuo and the crude product was purified by chromatography on silica gel (eluting with 2% methanol in chloroform) to afford the target product 10a as white solid (390 mg, yield 71%); mp 145–147 °C. HPLC-DAD: $t_r = 8.6$ min (% area = 97.9%). ^1H NMR (300 MHz, CDCl_3) δ 7.88 (d, $J = 7.29$ Hz, 1H), 7.35–7.22 (m, 8H), 6.83 (t, $J = 7.17$ Hz, 1H), 6.66–6.60 (m, 2H), 6.31 (d, $J = 7.29$ Hz, 1H), 6.09 (s, 1H), 4.56 (bs, 1H), 2.91–2.87 (m, 1H), 1.82 (s, 3H), 1.68 (s, 9H), 1.24 (d, $J = 6.81$ Hz, 6H). ^{13}C NMR (50 MHz, CDCl_3) δ 162.4, 155.2, 149.56, 145.84, 135.10, 133.95, 128.34, 127.76, 126.77, 118.69, 114.72, 113.59, 70.72, 61.80, 54.06, 33.74, 30.07, 29.68, 23.82. IR (KBr): 3425, 3321, 2935, 1613, 1517, 1380, 1219, 772 cm^{-1} . ESI-MS $\text{C}_{30}\text{H}_{35}\text{N}_7\text{O}$ (m/z): 510.0 ($\text{M}^+ + \text{H}$). HRMS: calcd, 510.2976 (MH^+); found, 510.2976 (MH^+).

Representative Procedure for the Synthesis of 2-(4-((Benzylamino)(1-tert-Butyl-1H-tetrazol-5-yl)methyl)phenyl)-2,3-dihydroquinazolin-4(1H)-one (11a). A solution of compound 3 (300 mg, 1.19 mmol), benzylamine (0.13 mL equiv, 1.19 mmol), and

tert-butyl isocyanide (0.13 mL, 1.61 mmol) was stirred in anhydrous methanol (5 mL) at rt for 10 min. Thereafter, trimethylsilyl azide (0.23 mL, 2.03 mmol) was added and the resulting mixture was further stirred for 6 h. On completion of the reaction (checked by TLC analysis), the methanol was removed in vacuo. The crude product was subjected to silica gel column chromatography using chloroform/methanol as mobile phase to afford the desired compound **11a** as white solid (410 mg, yield 74%); mp 120–122 °C. HPLC-DAD: t_r = 8.3 min (% area = 98.1%). ^1H NMR (300 MHz, CDCl_3) δ 7.85 (d, J = 6.78 Hz, 1H), 7.50 (d, J = 6.51 Hz, 2H), 7.29–7.19 (m, 8H), 6.84 (t, J = 7.44 Hz, 1H), 6.61 (d, J = 7.98 Hz, 1H), 5.88 (s, 1H), 5.81 (s, 1H), 5.21 (s, 1H), 4.38 (s, 1H), 3.78–3.73 (m, 1H), 3.64–3.60 (m, 1H), 1.45 (s, 9H). ^{13}C NMR (50 MHz, CDCl_3) δ 164.86, 155.22, 147.22, 140.37, 139.26, 138.65, 134.05, 128.74, 127.90, 127.4, 119.39, 115.45, 114.74, 68.23, 61.46, 56.64, 51.31, 29.92. IR (KBr): 3426, 3319, 2925, 1642, 1525, 1432, 1272, 771 cm^{-1} . ESI-MS $\text{C}_{27}\text{H}_{29}\text{N}_7\text{O}$ (m/z): 468.0 ($\text{M}^+ + \text{H}$). HRMS: calcd, 468.2506 (MH^+); found, 468.2518 (MH^+).

Experimental Section for Biology. Promastigote Viability Assay. The in vitro effects of the compounds on the growth of extracellular promastigotes were assessed as described previously.^{42a} The late log phase of *L. donovani* promastigotes (MHOM/IN/60/Dd₈, originally obtained from Imperial college, London) transfected with the firefly luciferase gene^{62,63} was seeded with complete M-199 medium at 5×10^4 /100 μL /well in 96-well plates and incubated with tested compounds for 96 h. Miltefosine and SSG were used as reference controls. After incubation, an aliquot (50 μL) of promastigote suspension was aspirated from each well of a 96-well plate and mixed with an equal volume of Steady Glo reagent (Promega) and luminescence was measured by a luminometer. The values were expressed as relative luminescence unit (RLU). The inhibition of parasitic growth is determined by comparison of the luciferase activity of compound treated parasites with that of untreated controls.

In Vitro Antiamastigote Assay. For assessing the activity of compounds against the amastigote stage of the parasite, murine macrophage cell line (J-774A.1) infected with promastigotes expressing luciferase firefly reporter gene was used. Cells were seeded in a 96-well plate (4×10^4 /100 μL /well) in RPMI-1640 containing 10% fetal calf serum and the plates were incubated at 37 °C in a CO_2 incubator. After 24 h, the medium was replaced with fresh medium containing stationary phase promastigotes (4×10^5 /100 μL /well) at the ratio of 1:10 (cell:promastigote). Promastigotes were phagocytized by the macrophages, and inside the phagolysosomes, they were transformed into amastigotes (nonmotile form). Each well of the plate was washed with plain RPMI medium after 24 h of incubation to remove the uninternalized promastigotes. The test compounds were added at 2-fold dilutions up to 7 points in complete medium starting from 40 μM concentration, and the plates were incubated at 37 °C in a CO_2 incubator for 72 h. After incubation, the drug containing medium was aspirated and 50 μL of PBS was added in each well and mixed with an equal volume of Steady Glo reagent. After gentle shaking for 1–2 min, the reading was taken in a luminometer.⁵¹ The values are expressed as relative luminescence units (RLU). Data were transformed into a graphic program (Excel). IC_{50} of antileishmanial activity was calculated by nonlinear regression analysis of the concentration response curve using the four parameter Hill equations.

Cytotoxicity Assay. The cell viability was determined using the MTT assay.⁵² As described previously, macrophage cells (J-774A.1 cell line) and mammalian kidney fibroblast cells, (Vero cell line) (1×10^5 cells/100 μL /well) were incubated with test compounds at seven concentrations starting from 400 μM . After 72 h of incubation, 25 μL of MTT reagent (5 mg/mL) in PBS medium was added to each well and incubated at 37 °C for 2 h. At the end of the incubation period, the supernatant were removed and 150 μL of pure DMSO was added to each well. After 15 min of shaking, the readings were recorded as absorbance at 544 nm on a microplate reader. The 50% cytotoxic concentration (CC_{50}) values were estimated as described by Huber & Koella.⁶⁴ The selectivity index (SI) for each compound was calculated as the ratio between cytotoxicity (CC_{50}) and activity (IC_{50}) against *Leishmania* amastigotes.

In Vivo Assay in *L. donovani*/Hamster Model. The in vivo antileishmanial activity was determined in golden hamsters (*Mesocricetus auratus*) infected with MHOM/IN/80/Dd₈ strain of *L. donovani*. The method as described by Gupta et al.⁵⁴ was used for in vivo evaluation. Golden hamsters (inbred strain) of either sex weighing 40–45 g were infected intracardially with 1×10^7 amastigotes per animal. After establishment of infection in 15–20 days, pretreatment spleen biopsy in all the animals was carried out to assess the degree of infection. The animals with +1 grade infection (5–10 amastigotes/100 spleen cell nuclei) were included in the chemotherapeutic trials. Five to six infected animals were randomized into several groups used for each test sample. Drug treatment (50 mg/kg) by intraperitoneal (IP) route was initiated after 2 days pretreatment of biopsy and continued for 5 consecutive days. Miltefosine and SSG were used as reference drugs. Post-treatment biopsies were done on day 7 of the last dose administration, and amastigote counts were assessed by Giemsa staining. Intensity of infection in both treated and untreated animals, and also the initial count in treated animals, was compared and the efficacy was expressed in terms of percentage inhibition (PI) using the following formula:

$$\text{PI} = 100 - [(\text{ANAT} \times 100)/(\text{INAT} \times \text{TIUC})]$$

Where PI is the percent inhibition of amastigotes multiplication, ANAT is the actual number of amastigotes in treated animals, INAT is the initial number of amastigotes in treated animals, and TIUC is time increase of parasites in untreated control animals.

Cytokines Assessment by ELISA. The level of various cytokines in the murine macrophages were measured using an OptEIA set ELISA kit (BD Biosciences, California, USA) according to manufacturer's instructions. Briefly, 1×10^6 murine macrophages (J-774A.1) infected with *Leishmania* amastigote (1:10 ratio) were incubated with tested compounds at IC_{50} concentration in 6-well plates. Supernatants were collected after 24 h for cytokines (IL-12, TNF- α , IL-10, and TGF- β) determination. The absorbance of the test samples was measured at 450 nm in an ELISA reader.

Nitric Oxide Production Assay. NO was quantified by the accumulation of nitrite in macrophage culture supernatant, and nitrite was detected by the Griess reaction as described by Kar et al.⁶⁵ Briefly, leishmania infected macrophage cells (1×10^6 /mL) were incubated with tested compounds for 24 h before nitrite assay. LPS (10 μg /mL) was used as a mitogen. Supernatant (500 μL) were collected after 24 h, mixed with an equal volume of Griess reagent (Sigma, USA) and left for 10 min at room temperature. The absorbance of the test samples was measured at 540 nm in an ELISA reader.

Statistical Analysis. Results were expressed as mean \pm SD from two independent experiments. The results were analyzed by one-way ANOVA followed by student's *t* test using GraphPad Prism (version 5.0) software.

■ ASSOCIATED CONTENT

⑤ Supporting Information

Final compounds characterization data, pharmacokinetics study, and material and methods of BSA interaction associated with this article. This material is available free of charge via the Internet at <http://pubs.acs.org>.

■ AUTHOR INFORMATION

Corresponding Author

*Phone: 91 522 2612411. Fax: +91 522 2623405. E-mail: prem_chauhan_2000@yahoo.com; premsc58@hotmail.com.

Notes

The authors declare no competing financial interest.

■ ACKNOWLEDGMENTS

We are grateful to Indian Council of Medical Research (M.S.) and Council of Scientific and Industrial Research (K.C.) for the financial support in the form of fellowship. We are also thankful to R. K. Purshottam and Tofan Kumar Rout for providing the

HPLC data and the SAIF Division of CDRI, Lucknow, for providing the spectroscopic data. CDRI communication no. 8453.

■ ABBREVIATIONS USED

BIOS, biology oriented synthesis; BSA, bovine serum albumin; IC₅₀, half maximal inhibitory concentration; IMCRs, isocyanides based multicomponent reactions; iNOS, inducible nitric oxide synthase; IP, intraperitoneally; PK, pharmacokinetics; SAR, structure–activity relationship; SSG, sodium stibogluconate; VL, visceral leishmaniasis

■ REFERENCES

- (1) Akopyants, N. S.; Kimblin, N.; Secundino, N.; Patrick, R.; Peters, N.; Lawyer, P.; Dobson, D. E.; Beverley, S. M.; Sacks, D. L. Demonstration of Genetic Exchange During Cyclical Development of Leishmania in the Sand Fly Vector. *Science* **2009**, *324*, 265–268.
- (2) WHO. *Working to Overcome the Global Impact of Neglected Tropical Diseases*; Stylus: Geneva, 2010. (b) Majumder, H. K. *Drug Targets in Kinetoplastid Parasites*; Springer Science+Business Media: New York, 2011.
- (3) Pimenta, P. F.; Turco, S. J.; McConville, M. J.; Lawyer, P. G.; Perkins, P. V.; Sacks, D. L. Stage-specific adhesion of Leishmania promastigotes to the sandfly midgut. *Science* **1992**, *256*, 1812–1815.
- (4) (a) Chappuis, F.; Sundar, S.; Hailu, A.; Ghalib, H.; Alvar, J.; Boelaer, M. Visceral leishmaniasis: what are the needs for diagnosis, treatment and control? *Nature Rev. Microbiol.* **2007**, *5*, 873–885. (b) Alvar, J.; Canavate, C.; Gutierrez- Solar, B.; Jimenez, M.; Lagnon, F.; Lopez-Velet, R.; Molina, R.; Moreno, J. Leishmania and human immunodeficiency virus coinfection: the first 10 years. *Clin. Microbiol. Rev.* **1997**, *10*, 298–319.
- (5) (a) Matte, C.; Maion, G.; Mourad, W.; Olivier, M. Leishmania donovani-induced macrophages cyclooxygenase-2 and prostaglandin E₂ synthesis. *Parasite Immunol.* **2001**, *23*, 177–184. (b) Bogdon, C.; Gessner, A.; Solbach, W.; Rollinghoff, M. Invasion, control and persistence of Leishmania parasites. *Curr. Opin. Immunol.* **1996**, *8*, 517–525.
- (6) (a) Sundar, S.; Rai, M. Advances in the treatment of leishmaniasis. *Curr. Opin. Infect. Dis.* **2002**, *15*, 593–598. (b) Pink, R.; Hudson, A.; Mouries, M. A.; Bendig, M. Opportunities and challenges in antiparasitic drug discovery. *Nature Rev. Drug Discovery* **2005**, *4*, 727–740.
- (7) (a) Berman, J. ABL: A New and Improved Amphotericin B for Visceral Leishmaniasis? *Am. J. Trop. Med. Hyg.* **2009**, *8*, 689–690. (b) Guerin, P. J.; Oliaro, P.; Sundar, S.; Boelaert, M.; Croft, S. L.; Desjeux, P.; Wasunna, K.; Bryceson, A. D. M. Visceral leishmaniasis: current status of control, diagnosis, and treatment, and a proposed research and development agenda. *Lancet Infect. Dis.* **2002**, *2*, 494–501.
- (8) (a) Poola, N. R.; Kalis, M.; Plakogiannis, F. M.; Taft, D. R. Characterization of pentamidine excretion in the isolated perfused rat kidney. *J. Antimicrob. Chemother.* **2003**, *52*, 397–404. (b) Dorlo, T. P. C.; Van Thiel, P. A. M.; Huitema, A. D. R.; Keizer, R. J.; De Vries, H. J. C.; Beijnen, J. H.; De Vries, P. J. Pharmacokinetics of Miltefosine in Old World Cutaneous Leishmaniasis Patients. *Antimicrob. Agents Chemother.* **2008**, *52*, 2855–2860. (c) Sindermann, H.; Engel, J. Development of miltefosine as an oral treatment for leishmaniasis. *Trans. R. Soc. Trop. Med. Hyg.* **2006**, *100* (Suppl 1), S17–S20.
- (9) (a) Croft, S. L.; Sundar, S.; Fairlam, A. H. Drug Resistance in Leishmaniasis. *Clin. Microbiol. Rev.* **2006**, *111*–126. (b) Sundar, S. Drug resistance in Indian visceral leishmaniasis. *Trop. Med. Int. Health* **2001**, *6*, 849–854.
- (10) Cavalli, A.; Bolognesi, M. L. Neglected tropical diseases: multitarget-directed ligands in the search for novel lead candidates against Trypanosoma and Leishmania. *J. Med. Chem.* **2009**, *52*, 7339–7359.
- (11) Meunier, B. Hybrid molecules with a dual mode of action: dream or reality? *Acc. Chem. Res.* **2008**, *41*, 69–77.
- (12) Congreve, M.; Chessari, G.; Tisi, D.; Woodhead, A. J. Recent developments in fragment-based drug discovery. *J. Med. Chem.* **2008**, *51*, 3661–3680.
- (13) Newman, D. J. Natural Products as Leads to Potential Drugs: An Old Process or the New Hope for Drug Discovery? *J. Med. Chem.* **2008**, *51*, 2589–2599.
- (14) (a) Breinbauer, R.; Vetter, I. R.; Waldmann, H. From protein domains to drug candidates—natural products as guiding principles in the design and synthesis of compound libraries. *Angew. Chem., Int. Ed.* **2002**, *41*, 2878–2890. (b) Basu, S.; Ellinger, B.; Rizzo, S.; Deraeve, C.; Schürmann, M.; Preut, H.; Arndt, H.-D.; Waldmann, H. Biology-oriented synthesis of a natural-product inspired oxepane collection yields a small molecule activator of the Wnt-pathway. *Proc. Natl. Acad. Sci. U. S. A.* **2011**, *108*, 6805–6810.
- (15) Tietze, L. F.; Bell, H. P.; Chandrasekhar, S. Natural Product Hybrids as New Leads for Drug Discovery. *Angew. Chem., Int. Ed.* **2003**, *42*, 3996–4028.
- (16) Wilson, R. M.; Danishefsky, S. J. Small molecule natural products in the discovery of therapeutic agents: the synthesis connection. *J. Org. Chem.* **2006**, *71*, 8329–8351.
- (17) Mhaske, S. B.; Argade, N. P. The chemistry of recently isolated naturally occurring quinazolinone alkaloids. *Tetrahedron* **2006**, *62*, 9787–9826.
- (18) Michael, J. P. Quinoline, quinazoline and acridone alkaloids. *Nat. Prod. Rep.* **2003**, *20*, 476–493.
- (19) (a) Bandekar, P. P.; Roopnarine, K. A.; Parekh, V. J.; Mitchell, T. R.; Novak, M. J.; Sinden, R. R. Antimicrobial Activity of Tryptanthrins in Escherichia coli. *J. Med. Chem.* **2010**, *53*, 3558–3565. (b) Bhattacharjee, A. K.; Skanchy, D. J.; Jennings, B.; Hudson, T. H.; Brendle, J. J.; Werbovetz, K. A. Analysis of stereoelectronic properties, mechanism of action and pharmacophore of synthetic indolo[2,1-b]quinazoline-6,12-dione derivatives in relation to antileishmanial activity using quantum chemical, cyclic voltammetry and 3-D-QSAR CATALYST procedures. *Bioorg. Med. Chem.* **2002**, *10*, 1979–1989.
- (20) Chiou, W.; Liao, J.; Chen, C. Comparative Study on the Vasodilatory Effects of Three Quinazoline Alkaloids Isolated from Evodia rutaecarpa. *J. Nat. Prod.* **1996**, *59*, 374–378.
- (21) Liang, J. L.; Cha, H. C.; Jahng, Y. Recent Advances in the Studies on Luotonins. *Molecules* **2011**, *16*, 4861–4883.
- (22) (a) Chinigo, G. M.; Paige, M.; Grindrod, S.; Hamel, E.; Dakshanamurthy, S.; Chruszcz, M.; Minor, W.; Brown, M. L. Brown Asymmetric Synthesis of 2,3-Dihydro-2-arylquinazolin-4-ones: Methodology. Application to a Potent Fluorescent Tubulin Inhibitor with Anticancer Activity. *J. Med. Chem.* **2008**, *51*, 4620–4631. (b) El-Azab, A. S.; ElTahir, K. E. H. Design and synthesis of novel 7-aminoquinazoline derivatives: antitumor and anticonvulsant activities. *Bioorg. Med. Chem. Lett.* **2012**, *22*, 1879–1885. (c) Saravanan, G.; Alagarsamy, V.; Prakash, C. R. Design, synthesis and anticonvulsant activities of novel 1-(substituted/unsubstituted benzylidene)-4-(4-(6,8-dibromo-2-(methyl/phenyl)-4-oxoquinazolin-3(4H)-yl)phenyl) semicarbazide derivatives. *Bioorg. Med. Chem. Lett.* **2012**, *22*, 3072–3078.
- (23) Wang, Z.; Wang, M.; Yao, X.; Li, Y.; Tan, J.; Wang, L.; Qiao, W.; Geng, Y.; Liu, Y.; Wang, Q. Design, synthesis and antiviral activity of novel quinazolinones. *Eur. J. Med. Chem.* **2012**, *53*, 275–282.
- (24) (a) Abbas, S. E.; Awadallah, F. M.; Ibrahim, N. A.; Said, E. G.; Kamel, G. M. New quinazolinone–pyrimidine hybrids: synthesis, anti-inflammatory, and ulcerogenicity studies. *Eur. J. Med. Chem.* **2012**, *53*, 141–149. (b) Amin, K. M.; Kamel, M. M.; Anwar, M. M.; Khedr, M.; Syam, Y. M. Synthesis, biological evaluation and molecular docking of novel series of spiro[2H,3H]quinazoline-2,10-cyclohexan]-4(1H)-one derivatives as anti-inflammatory and analgesic agents. *Eur. J. Med. Chem.* **2010**, *45*, 2117–2131.
- (25) (a) Al-Omary, F. A. M.; Abou-zeid, L. A.; Nagi, M. N.; Habib, E. E.; Abdel-Aziz, A. M.; El-Azab, A. S.; Abdel-Hamide, S. G.; Al-Omar, M. A.; Al-Obaid, A. M.; El-Subbagh, H. I. Non-classical antifolates. Part 2: Synthesis, biological evaluation, and molecular modeling study of some new 2,6-substituted-quinazolin-4-ones. *Bioorg. Med. Chem. Lett.* **2010**, *18*, 2849–2863. (b) Suresha, G. P.; Suhas, R.; Kapfo, W.; Gowda, D. C. Urea/thiourea derivatives of quinazolinone lysine conjugates: synthesis

and structure–activity relationships of a new series of antimicrobials. *Eur. J. Med. Chem.* **2011**, *46*, 2530–2540.

(26) Mohameda, M. S.; Kamel, M. M.; Kassem, E. M. M.; Abotaleb, N.; AbdEl-moez, S. I.; Ahmeda, M. F. Novel 6,8-dibromo-4(3H)-quinazolinone derivatives of anti-bacterial and anti-fungal activities. *Eur. J. Med. Chem.* **2010**, *45*, 3311–3319.

(27) Gemma, S.; Camodeca, C.; Brindisi, M.; Brogi, S.; Kukreja, G.; Kunjir, S.; Gabellieri, E.; Lucantoni, L.; Habluetzel, A.; Taramelli, D.; Basilio, N.; Gualdani, R.; Tadini-Buoninsegni, F.; Bartolommei, G.; Moncelli, M. R.; Martin, R. E.; Summers, R. L.; Lamponi, S.; Savini, L.; Fiorini, L.; Valoti, M.; Novellino, E.; Campiani, G.; Butini, S. Mimicking the Intramolecular Hydrogen Bond: Synthesis, Biological Evaluation, and Molecular Modeling of Benzoxazines and Quinazolines as Potential Antimalarial Agents. *J. Med. Chem.* **2012**, *55*, 10387–10404.

(28) Rudolph, J.; Esler, W. P.; O'Connor, S.; Coish, P. D. G.; Wickens, P. L.; Brands, M.; Bierter, D. E.; Bloomquist, B. T.; Bondar, G.; Chen, L.; Chuang, C.; Claus, T. H.; Fathi, Z.; Fu, W.; Khire, U. R.; Kristie, J. A.; Liu, X.; Lowe, D. B.; McClure, A. C.; Michels, M.; Ortiz, A.; Ramsden, P. D.; Schoenleber, R. W.; Shelekhn, T. E.; Vakalopoulos, A.; Wang, L.; Yi, L.; Gardell, S. J.; Livingston, J. N.; Sweet, L. J.; Bullock, W.; Quinazolinone, H. Derivatives as Orally Available Ghrelin Receptor Antagonists for the Treatment of Diabetes and Obesity. *J. Med. Chem.* **2007**, *50*, S202–S216.

(29) Rhee, H.; Yoo, J. H.; Lee, E.; Kwon, Y. J.; Seo, H.; Lee, Y.; Choo, H. P. Synthesis and cytotoxicity of 2-phenylquinazolin-4(3H)-one derivatives. *Eur. J. Med. Chem.* **2011**, *46*, 3900–3908.

(30) Ismail, M. A. H.; Barker, S.; Abou El Ella, D. A.; Abouzid, K. A. M.; Toubar, R. A.; Todd, M. H. Design and Synthesis of New Tetrazolyl- and Carboxy-biphenylmethyl-quinazolin-4-one Derivatives as Angiotensin II AT1 Receptor Antagonists. *J. Med. Chem.* **2006**, *49*, 1526–1535.

(31) Sharma, M.; Pandey, S.; Chauhan, K.; Sharma, D.; Kumar, B.; Chauhan, P. M. S. Cyanuric chloride catalyzed mild protocol for synthesis of biologically active dihydro/spiro quinazolinones and quinazolinone-glycoconjugates. *J. Org. Chem.* **2012**, *77*, 929–937.

(32) Costa, E. V.; Pinheiro, M. L. B.; Xavier, C. M.; Silva, J. R. A.; Amaral, A. F.; Souza, A. D. L.; Barison, A.; Campos, F. R.; Ferreira, A. G.; Machado, G. M. C.; Leon, L. P. L. A Pyrimidine- β -carboline and Other Alkaloids from *Annona foetida* with Antileishmanial Activity. *J. Nat. Prod.* **2006**, *69*, 292–294.

(33) Akue-Gedu, R.; Debiton, E.; Ferandin, Y.; Meijer, L.; Prudhomme, M.; Anizon, F.; Moreau, P. Synthesis and biological activities of aminopyrimidyl-indoles structurally related to meridianins. *Bioorg. Med. Chem.* **2009**, *17*, 4420–4424.

(34) Sanchez, L. M.; Lopez, D.; Vesely, B. A.; Togna, G. D.; Gerwick, W. H.; Kyle, D. E.; Linington, R. G.; Almiramides, A-C Discovery and Development of a New Class of Leishmaniasis Lead Compounds. *J. Med. Chem.* **2010**, *53*, 4187–4197.

(35) Balasegaram, M.; Young, H.; Chappuis, F.; Priotto, G.; Raguenaud, M. E.; Checchi, F. Effectiveness of melarsoprol and eflornithine as first-line regimens for gambiense sleeping sickness in nine Médecins Sans Frontières programmes. *Trans R. Soc. Trop. Med. Hyg.* **2009**, *103*, 280–290.

(36) (a) Muh, U.; Schuster, M.; Heim, R.; Singh, A.; Olson, E. R.; Greenberg, E. P. Novel *Pseudomonas aeruginosa* Quorum-Sensing Inhibitors Identified in an Ultra-High-Throughput Screen. *Antimicrob. Agents Chemother.* **2006**, *50*, 3674–3679. (b) Vitale, C.; Mercurio, G.; Castiglioni, C.; Cornoldi, A.; Tulli, A.; Fini, M.; Volterrani, M.; Rosano, G. M. C. Metabolic effect of telmisartan and losartan in hypertensive patients with metabolic syndrome. *Cardiovasc. Diabetol.* **2005**, *4*, 6–13.

(37) Sivaprakasam, P.; Tosso, P. N.; Doerksen, R. J. Structure–Activity Relationship and Comparative Docking Studies for Cycloguanil Analogs as Pf DHFR-TS Inhibitors. *J. Chem. Inf. Model.* **2009**, *49*, 1787–1796. (b) Rastelli, G.; Sirawaraporn, W.; Sompornpisut, P.; Vilaivan, T.; Kamchonwongpaisan, S.; Quarrell, R.; Lowe, G.; Thebtaranonth, Y.; Yuthavong, Y. Interactions of pyrimethamine, cycloguanil and WR99210 and their analogues with *Plasmodium falciparum* dihydrofolate reductase: structural basis for antifolate resistance. *Bioorg. Med. Chem.* **2000**, *8*, 1117–1128.

(38) (a) Torrence, P. F.; Fan, X.; Zhanga, X.; Loiseau, P. M. Structurally diverse 5-substituted pyrimidine nucleosides as inhibitors of *Leishmania donovani* promastigotes in vitro. *Bioorg. Med. Chem. Lett.* **2006**, *16*, 5047–5051. (b) Musonda, C. C.; Whitlock, G. A.; Witty, M. J.; Brun, R.; Kaiser, M. Synthesis and evaluation of 2-pyridyl pyrimidines with in vitro antiparasitoid and antileishmanial activity. *Bioorg. Med. Chem. Lett.* **2009**, *19*, 401–405. (c) Determann, R.; Dreher, J.; Baumann, K.; Preu, L.; Jones, P. G.; Totzke, F.; Schachte, C.; Kubbutat, M. H. G.; Kunick, C. 2-Anilino-4-(benzimidazol-2-yl)-pyrimidines A multikinase inhibitor scaffold with antiproliferative activity toward cancer cell lines. *Eur. J. Med. Chem.* **2012**, *53*, 254–263.

(39) (a) Smith, A. L.; D'Angelo, N. D.; Bo, Y. Y.; Booker, S. K.; Cee, V. J.; Herberich, B.; Hong, F.; Jackson, C. L. M.; Lanman, B. A.; Liu, L.; Nishimura, N.; Pettus, L. H.; Reed, A. B.; Tadesse, S.; Tamayo, N. A.; Wurz, R. P.; Yang, K.; Andrews, K. L.; Whittington, D. A.; McCarter, J. D.; Miguel, T. S.; Zalameda, L.; Jiang, J.; Subramanian, R.; Mullady, E. L.; Caenepeel, S.; Freeman, D. J.; Wang, L.; Zhang, N.; Wu, T.; Hughes, P. E.; Norman, M. H. Structure-Based Design of a Novel Series of Potent, Selective Inhibitors of the Class I Phosphatidylinositol 3-Kinases. *J. Med. Chem.* **2012**, *55*, 5188–5219. (b) Menicagli, R.; Samaritani, S.; Signore, G.; Vaglini, F.; Via, L. D. In Vitro Cytotoxic Activities of 2-Alkyl-4,6-diheteroalkyl-1,3,5-triazines: New Molecules in Anticancer Research. *J. Med. Chem.* **2004**, *47*, 4649–4652. (c) Gravestock, D.; Rousseau, A. L.; Lourens, A. C. U.; Moleele, S. S.; Zyl, R. L. V.; Steenkamp, P. A. Expedient synthesis and biological evaluation of novel 2,N⁶-disubstituted 1,2-dihydro-1,3,5-triazine-4,6-diamines as potential antimalarials. *Eur. J. Med. Chem.* **2011**, *46*, 2022–2030. (d) Vidal-Mosquera, M.; Fernandez-Carvajal, A.; Moure, A.; Valente, P.; Planells-Cases, R.; Gonzalez-Ros, J. M.; Bujons, J.; Ferrer-Montiel, A.; Messegue, A. Triazine-Based Vanilloid 1 Receptor Open Channel Blockers: Design, Synthesis, Evaluation, and SAR Analysis. *J. Med. Chem.* **2011**, *54*, 7441–7452.

(40) (a) Okandeji, B. O.; Greenwald, D. M.; Wroten, J.; Sello, J. K. Synthesis and evaluation of inhibitors of bacterial drug efflux pumps of the major facilitator superfamily. *Bioorg. Med. Chem.* **2011**, *19*, 7679–7689. (b) Noren-Muller, A.; Reis-Correa, I., Jr.; Prinz, H.; Rosenbaum, C.; Saxena, K.; Schwalbe, H. J.; Vestweber, D.; Cagna, G.; Schunk, S.; Schwarz, O.; Schiewe, H.; Waldmann, H. Discovery of protein phosphatase inhibitor classes by biology-oriented synthesis. *Proc. Natl. Acad. Sci. U. S. A.* **2006**, *103*, 10606–10611. (c) Sutherland, H. S.; Blaser, A.; Kmentova, I.; Franzblau, S. G.; Wan, B.; Wang, Y.; Ma, Z.; Palmer, B. D.; Denny, W. A.; Thompson, A. M. Synthesis and structure–activity relationships of antitubercular 2-nitroimidazooxazines bearing heterocyclic side chains. *J. Med. Chem.* **2010**, *53*, 855–866. (d) Semple, G.; Skinner, P. J.; Gharbaoui, T.; Shin, Y.; Jung, J.; Cherrier, M. C.; Webb, P. J.; Tamura, S. Y.; Boatman, P. D.; Sage, C. R.; Schrader, T. O.; Chen, R.; Colletti, S. L.; Tata, J. R.; Waters, M.; Cheng, K.; Taggart, A. K.; Cai, T.; Carballo-Jane, E.; Behan, D. P.; Connolly, D. T.; Richman, J. G. 3-(1H-Tetrazol-5-yl)-1,4,5,6-tetrahydro-cyclopentapyrazole (MK-0354): A Partial Agonist of the Nicotinic Acid Receptor, G-Protein Coupled Receptor 109a, with Antipolytic but No Vasodilatory Activity in Mice. *J. Med. Chem.* **2008**, *51*, 5101–5108. (e) Biot, C.; Bauer, H.; Schirmer, R. H.; Davioud-Charvet, E. 5-Substituted Tetrazoles as Bioisosteres of Carboxylic Acids. Bioisosterism and Mechanistic Studies on Glutathione Reductase Inhibitors as Antimalarials. *J. Med. Chem.* **2004**, *47*, 5972–5983. (f) Fan, X.; Zhang, X.; Bories, C.; Loiseau, P. M.; Torrence, P. F. The Ugi reaction in the generation of new nucleosides as potential antiviral and antileishmanial agents. *Bioorg. Med. Chem.* **2007**, *35*, 121–136.

(41) (a) Sunduru, N.; Agarwal, A.; Katiyar, S. B.; Shukla, N.; Goyal, N.; Gupta, S.; Chauhan, P. M. S. Synthesis of 2,4,6 trisubstituted pyrimidine and triazine heterocycles as antileishmanial agents. *Bioorg. Med. Chem.* **2006**, *14*, 7706–7715. (b) Kumar, A.; Katiyar, S. B.; Gupta, S.; Chauhan, P. M. S. Syntheses of new substituted triazino tetrahydroisoquinolines and β -carboline as novel antileishmanial agents. *Eur. J. Med. Chem.* **2006**, *41*, 106–113. (c) Sunduru, N.; Palne, S.; Chauhan, P. M. S.; Gupta, S. Synthesis and antileishmanial activity of novel 2,4,6-trisubstituted pyrimidines 1,3,5-triazines. *Eur. J. Med. Chem.* **2009**, *44*, 2473–2481. (d) Gupta, L.; Sunduru, N.; Verma, A.; Srivastava, S.; Gupta, S.; Goyal, N.; Chauhan, P. M. S. Synthesis and biological

evaluation of new [1,2,4]triazino[5,6-*b*]indol-3-ylthio-1,3,5-triazines and [1,2,4]triazino[5,6-*b*]indol-3-ylthio-pyrimidines against *Leishmania donovani*. *Eur. J. Med. Chem.* **2010**, *45*, 2359–2365.

(42) (a) Porwal, S.; Chauhan, S. S.; Chauhan, P. M. S.; Shakya, N.; Verma, A.; Gupta, S. Discovery of Novel Antileishmanial Agents in an Attempt to Synthesize Pentamidine–Aplysinopsin Hybrid Molecule. *J. Med. Chem.* **2009**, *19*, 5793–5802. (b) Sharma, M.; Chauhan, K.; Chauhan, S. S.; Kumar, A.; Singh, S. V.; Saxena, J. K.; Agarwal, P.; Srivastava, K.; Kumar, S. R.; Puri, S. K.; Shah, P.; Siddiqi, M. I.; Chauhan, P. M. S. Synthesis of hybrid 4-anilinoquinoline triazines as potent antimalarial agents, their in silico modeling and bioevaluation as *Plasmodium falciparum* transketolase and β -hematin inhibitors. *Med. Chem. Commun.* **2012**, *3*, 71–79. (c) Sharma, M.; Chaturvedi, V.; Manju, Y. K.; Bhatnagar, S.; Srivastava, K.; Puri, S. K.; Chauhan, P. M. S. Substituted quinolinyl chalcones and quinolinyl pyrimidines as a new class of anti-infective agents. *Eur. J. Med. Chem.* **2009**, *44*, 2081–2091. (d) Sunduru, N.; Sharma, M.; Srivastava, K.; Kumar, S. R.; Puri, S. K.; Saxena, J. K.; Chauhan, P. M. S. Synthesis of oxalamide and triazine derivatives as a novel class of hybrid 4-aminoquinoline with potent antiparasitodal activity. *Bioorg. Med. Chem.* **2009**, *17*, 6451–6462. (e) Katiyar, S. B.; Srivastava, K.; Puri, S. K.; Chauhan, P. M. S. Synthesis of 2-[3,5-substituted pyrazol-1-yl]-4,6-trisubstituted triazine derivatives as antimalarial agents. *Bioorg. Med. Chem. Lett.* **2005**, *15*, 4957–4960. (f) Kumar, A.; Srivastava, K.; Kumar, S. R.; Puri, S. K.; Chauhan, P. M. S. Synthesis and bioevaluation of hybrid 4-aminoquinoline triazines as a new class of antimalarial agents. *Bioorg. Med. Chem. Lett.* **2008**, *18*, 6530–6533. (g) Tyagi, V.; Khan, S.; Shivhare, R.; Srivastava, K.; Gupta, S.; Kidwai, S.; Srivastava, K.; Puri, S. K.; Chauhan, P. M. S. A natural product inspired hybrid approach towards the synthesis of novel pentamidine based scaffolds as potential anti-parasitic agents. *Bioorg. Med. Chem. Lett.* **2013**, *23*, 291–296.

(43) Dockal, M.; Carter, D. C.; Ruker, F. Five recombinant fragments of human serum albumin—tools for the characterization of the warfarin binding site. *J. Biol. Chem.* **2000**, *275*, 3042–3050.

(44) Tian, J. N.; Liu, J. Q.; Zhang, J. Y.; Hu, Z. D.; Chen, X. G. Fluorescence Studies on the Interactions of Barbaloin with Bovine Serum Albumin. *Chem. Pharm. Bull.* **2003**, *51*, 579–582.

(45) Ran, D. H.; Wu, X.; Zheng, J. H.; Yang, J. H.; Zhou, H. P.; Zhang, M. F.; Tang, Y. J. Study on the interaction between florasulam and bovine serum albumin. *J. Fluoresc.* **2007**, *17*, 721–726.

(46) Kun, R.; Kis, L.; Dekany, I. Hydrophobization of bovine serum albumin with cationic surfactants with different hydrophobic chain length. *Colloids Surf., B* **2010**, *79*, 61–68.

(47) Liu, B.; Guo, Y.; Wang, J.; Xu, R.; Wang, X.; Wang, D.; Zhang, L. Q.; Xu, Y. N. Spectroscopic studies on the interaction and sonodynamic damage of neutral red (NR) to bovine serum albumin (BSA). *J. Luminesc.* **2010**, *130*, 1036–1043.

(48) Xiang, G. H.; Tong, C. L.; Lin, H. Z. Nitroaniline isomers interaction with bovine serum albumin and toxicological implications. *J. Fluoresc.* **2007**, *17*, 512–521.

(49) Wattanasin, S.; Murphy, W. S. An improved procedure for the preparation of chalcones and related enones. *Synthesis* **1980**, *8*, 647–650.

(50) (a) Domling, A.; Wang, W.; Wang, K. Chemistry and Biology of Multicomponent Reactions. *Chem. Rev.* **2012**, *112*, 3083–3135. (b) Domling, A.; Beck, B.; Magnin-Lachaux, M. 1-Isocyanomethylbenzotriazole and 2,2,4,4-tetramethylbutylisocyanide-cleavable isocyanides useful for the preparation of α -aminomethyl tetrazoles. *Tetrahedron Lett.* **2006**, *47*, 4289–4291.

(51) Gupta, L.; Talwar, A.; Shakya, N.; Palne, S.; Gupta, S.; Chauhan, P. M. S. Synthesis of marine alkaloid: 8,9-dihydrococcinamide B and its analogues as novel class of antileishmanial agents. *Bioorg. Med. Chem. Lett.* **2007**, *17*, 4075–4079.

(52) (a) Mosmann, T. Rapid colorimetric assay for cellular growth and survival: application to proliferation and cytotoxicity assays. *J. Immunol. Methods* **1983**, *65*, 55–63. (b) Carmichael, J.; DeGraff, W. G.; Gazdar, A. F.; Minna, J. D.; Mitchel, J. B. Evaluation of a tetrazolium-based semiautomated colorimetric assay: assessment of radiosensitivity. *Cancer Res.* **1987**, *47*, 943–946.

(53) Gupta, S.; Ramesh; Sharma, S. C.; Srivastava, V. M. L. Efficacy of picroliv combination with miltefosine, an orally effective antileishmanial drug against experimental visceral leishmaniasis. *Acta Trop.* **2005**, *94*, 41–47.

(54) (a) Talancon, D.; Bosque, R.; Lopez, C. Study of the Effect Induced by the Substituents on the Ring–Chain Tautomerism of Schiff Bases Derived from Norephedrine. *J. Org. Chem.* **2010**, *75*, 3294–3300. (b) Dubar, F.; Anquetin, G.; Pradines, B.; Dive, D.; Khalife, J.; Biot, C. Enhancement of the Antimalarial Activity of Ciprofloxacin Using a Double Prodrug/Bioorganometallic Approach. *J. Med. Chem.* **2009**, *52*, 7954–7957. (c) Bellot, F.; Cosledan, F.; Vendier, L.; Brocard, J.; Meunier, B.; Robert, A. Trioxaferroquines as New Hybrid Antimalarial Drugs. *J. Med. Chem.* **2010**, *53*, 4103–4109.

(55) Lakowicz, J. R. *Principles of Fluorescence Spectroscopy*, 3rd ed.; Springer: New York, 2006; pp 11–12.

(56) Lakowicz, J. R.; Weber, G. Quenching of fluorescence by oxygen, a probe for structural fluctuations in macromolecules. *Biochemistry* **1973**, *12*, 4161–4170.

(57) Maurice, R. E.; Camillo, A. G. Fluorescence quenching studies with proteins. *Anal. Biochem.* **1981**, *114*, 199–212.

(58) Jayabharathi, J.; Thanikachalam, V.; Sathishkumar, R.; Jayamoorthy, K. Fluorescence investigation of the interaction of 2-(4-fluorophenyl)-1-phenyl-1H-phenanthro[9,10-*d*]imidazole with bovine serum albumin. *J. Photochem. Photobiol., B: Biol.* **2012**, *117*, 222–228.

(59) Lehrer, S. S. Solute perturbation of protein fluorescence. The quenching of the tryptophyl fluorescence of model compounds and of lysozyme by iodide ion. *Biochemistry* **1971**, *10*, 3254–3263.

(60) Gong, A.; Zhu, X.; Hu, Y.; Yu, S. A fluorescence spectroscopic study of the interaction between epristeride and bovin serum albumin and its analytical application. *Talanta* **2007**, *73*, 668–673.

(61) Yamaoka, K.; Nakagawa, T.; Uno, T. Application of a Akaike's information criterion (AIC) in the evaluation of linear pharmacokinetic equations. *J. Pharmacokinet. Biopharm.* **1978**, *6*, 65–175.

(62) Davies, B.; Morris, T. Physiological parameters in laboratory animals and humans. *Pharm. Res.* **1993**, *10*, 1093–1095.

(63) Gupta, A. S. R.; Sundar, S.; Goyal, N. Use of *Leishmania donovani* Field Isolates Expressing the Luciferase Reporter Gene in in Vitro Drug Screening. *Antimicrob. Agents Chemother.* **2005**, *49*, 3776–3783.

(64) (a) Huber, W.; Koella, J. C. A comparison of three methods of estimating EC₅₀ in studies of drug resistance of malaria parasites. *Acta Trop.* **1993**, *55*, 257–261.

(65) Kar, S.; Sharma, G.; Das, P. K. Fucoidan cures infection with both antimony-susceptible and -resistant strains of *Leishmania donovani* through Th1 response and macrophage-derived oxidants. *J. Antimicrob. Chemother.* **2011**, *66*, 618–625.

■ NOTE ADDED AFTER ASAP PUBLICATION

This paper was published on the Web on May 7, 2013, with an error to the Abstract graphic. The corrected version was reposted May 16, 2013.